uOttawa

L'Université canadienne
Canada's university

FACULTÉ DES ÉTUDES SUPÉRIEURES ET POSTOCTORALES

uOttawa

L'Université canadienne
Canada's university

FACULTY OF GRADUATE AND POSDOCTORAL STUDIES

Dan Rudkevitch

AUTEUR DE LA THÈSE / AUTHOR OF THESIS

M.A.Sc. (Chemical Engineering)

GRADE / DEGREE

Department of Chemical Engineering

FACULTÉ, ÉCOLE, DÉPARTEMENT / FACULTY, SCHOOL, DEPARTMENT

Similitude of a High Pressure Three-Phase Fluidized Bed Subject to Foaming

TITRE DE LA THÈSE / TITLE OF THESIS

Dr. Arturo Macchi

DIRECTEUR (DIRECTRICE) DE LA THÈSE / THESIS SUPERVISOR

CO-DIRECTEUR (CO-DIRECTRICE) DE LA THÈSE / THESIS CO-SUPERVISOR

EXAMINATEURS (EXAMINATRICES) DE LA THÈSE / THESIS EXAMINERS

Dr. Christopher Lan

Dr. Poupak Mehrani

Gary W. Slater

Le Doyen de la Faculté des études supérieures et postdoctorales / Dean of the Faculty of Graduate and Postdoctoral Studies

Similitude of a High Pressure Three-Phase Fluidized Bed Subject to Foaming

By

Dan Rudkevitch

Thesis submitted to the
Faculty of Graduate and Postdoctoral Studies
In partial fulfillment of the requirements
For the Master of Applied Science in Chemical Engineering

Department of Chemical Engineering
University of Ottawa

Your file Votre référence
ISBN: 978-0-494-49272-7
Our file Notre référence
ISBN: 978-0-494-49272-7

Abstract

Most hydrodynamic models for gas-liquid-solid fluidized beds are developed for atmospheric pressure and they assume that the liquid physical properties, including density, viscosity and surface tension, are sufficient to characterize bubble dynamics. While true for mono-component liquids, multi-component liquids display bubble coalescence inhibition. It is postulated that the hydrodynamic features of a three-phase fluidized bed can be scaled based on geometric similarity and dimensional similitude by matching five dimensionless groups: a liquid Reynolds Number, $Re_L = U_L d_P \rho_L / \mu_L$; an Archimedes Number, $Ar_p = \rho_L g d_P^3 (\rho_L - \rho_G) / \mu_L^2$; a gas-liquid density ratio, ρ_G/ρ_L; a particle-liquid density ratio, ρ_p/ρ_L; and a superficial velocity ratio, U_G/U_L. A bubble coalescence index, I, (1 for mono-component liquids and 2 for multi-component liquids) is an empirical means to account for bubble coalescence inhibition. The effects of pressure and surfactants on the hydrodynamics of three-phase fluidized beds, including the phase holdups, dispersed to coalesced bubbling regime transition velocity and minimum liquid fluidization velocity, are evaluated with water and a 0.5%wt aqueous ethanol solution, nitrogen gas, and 2 mm glass beads operated at pressures of 0.1 to 6 MPa The effect of pressure on the bed phase holdups, in particular the gas holdup, is significant and more pronounced at larger gas flow rates where pressure has a greater effect on the equilibrium bubble size. The addition of ethanol significantly increases the gas holdup and then as pressure is increased, the phase holdups remain relatively constant. The gas holdups in the bed are always lower than those in the freeboard region. Pressure and surfactants both delay the transition from the dispersed to coalesced bubbling regime, more so for the latter.

Sommaire

La plupart des corrélations et modèles hydrodynamiques pour les lits fluidisés gaz-liquide-solide sont valident à pression atmosphérique, et elles supposent que les principales propriétés physiques du liquide, la densité, la viscosité, et la tension superficielle, sont suffisantes pour caractériser la dynamique des bulles. Cela vaut pour les liquides purs, mais les mélanges liquides montrent une inhibition de coalescence de bulles. On postule que l'hydrodynamique des lits fluidisés triphasées peut être modélisée par l'analyse dimensionnelle en assurant la similitude géométrique et l'égalité de cinq groupes adimensionnels: le nombre de Reynolds, $Re_L = U_L d_P \mu_L / \rho_L$; le nombre d'Archimède, $Ar_p = \rho_L g d_P^3 (\rho_L - \rho_G) / \mu_L^2$; un rapport de densité de gaz-liquide, ρ_G/ρ_L; un rapport plein de densité solide-liquide, ρ_S/ρ_L; et un rapport de vitesse superficielle, U_G/U_L. Un index de coalescence, I, (1 pour les liquides purs et 2 pour les mélanges) est un moyen empirique pour caractériser l'inhibition de coalescence de bulles. Les effets de pression et surfactants sur les rétentions de phases, la vitesse de transition entre les régimes à bulles dispersées et coalescentes, et la vitesse liquide minimum de fluidisation sont évaluées avec de l'eau et une solution aqueuse d'éthanol 0.5%wt, de l'azote, et des billes de verre de 2 mm de diamètre à des pressions de 0.1 à 6 MPa. L'effet de pression sur les rétentions de phases dans le lit, en particulier celle du gaz, est significatif et plus prononcé aux plus grands débits de gaz, où la pression a plus d'effet sur la taille des bulles à l'équilibre. L'addition d'éthanol augmente de manière significative la rétention du gaz, et à mesure que de la pression est augmentée, les rétentions de phases demeurent constantes. Les rétentions de gaz dans le lit sont inférieures à celles dans la région gaz-liquide au dessus du lit. La pression et les surfactants retardent la transition entre les régimes à bulles dispersés et coalescentes.

Table of Contents

List of Tables

List of Figures

Acknowledgements

I would like to first express my gratitude to Dr. Arturo Macchi for his support, guidance and inspiration. He has made this a truly enjoyable experience.

I would like to thank all of those directly and indirectly involved in this work; Louis, Franco, and Gérard for their countless hours working with the system.

Finally, I would like to thank my family and friends who have supported me during my studies.

Chapter 1 – Introduction

Multiphase reactors are vessels in which two or more phases (gas, liquid or solid) come into contact with each other. Three-phase fluidized beds are employed when intimate contact between solid, liquid and gas phases is required. Industrial applications of three-phase fluidized beds include flue gas desulphurization, hydrotreating of resides, fermentation, aerobic biological wastewater treatment, Fischer-Tropsch synthesis, and coal gasification (Fan, 1989). The three-phase fluidized bed in this thesis is configured to have the liquid and gas flowing co-currently through a stagnant bed of particles, depicted in Figure 1.1. The liquid is the continuous phase and the gas and solid are the dispersed phases. In this case, the predominant interaction occurs between the gas bubbles and the surrounding liquid-solid suspension.

Three distinct regions exist in a three-phase fluidized bed: the distributor region, the bulk region, and the freeboard region. The distributor region exists directly above the gas and liquid distributors. Gas bubbles are formed and the bubble develops its final shape in the distributor region. The bulk region of the fluidized bed constitutes the main portion of the bed. The freeboard region is situated above the bulk region and consists of mainly gas and liquid. Small amounts of particles can be entrained in the wakes of bubbles in the bulk region of the bed and carried into the freeboard region. Above a certain column height, known as the transport disengagement height, there are no particles. The bed height, which is the interface between the bulk and freeboard regions, is much more distinct for large/heavy particle systems than for small/light particle systems (Fan, 1989).

Reactor geometry, physical properties and operating conditions influence the hydrodynamics of multiphase reactors. The hydrodynamics can be characterized by the bubble characteristics (size and size distribution, shape and rise velocity) and the phase holdups (volumetric phase fractions). Bubble dynamics also dictate the flow regime. There are three flow regimes associated with three-phase fluidized beds: the dispersed bubbling regime, the coalesced bubbling regime, and the slug flow regime. The dispersed bubbling regime exists at low gas velocities and is characterized by small,

uniform bubbles dispersed across the entire cross section of the column. The bubbles in the dispersed bubbling regime rise in an organized manner, and there is no bubble coalescing present. The addition of more gas primarily results in an increase in bubble population, rather than bubble size. This regime cannot be indefinitely sustained as eventually bubbles will start to coalesce. The coalesced bubbling regime exists at larger gas velocities and is characterized by a wide bubble size distribution, ranging from a few millimetres to a couple centimetres. The larger bubbles tend to travel faster than the smaller bubbles; hence there is significant backmixing of the liquid and strong liquid circulation patterns. The slug flow regime is present in small columns with an inner diameter less than 0.1 m. It is observed at high gas velocities and the bubbles have a diameter with the same order of magnitude as the column as a result of the walls stabilizing the bubbles as they increase in size.

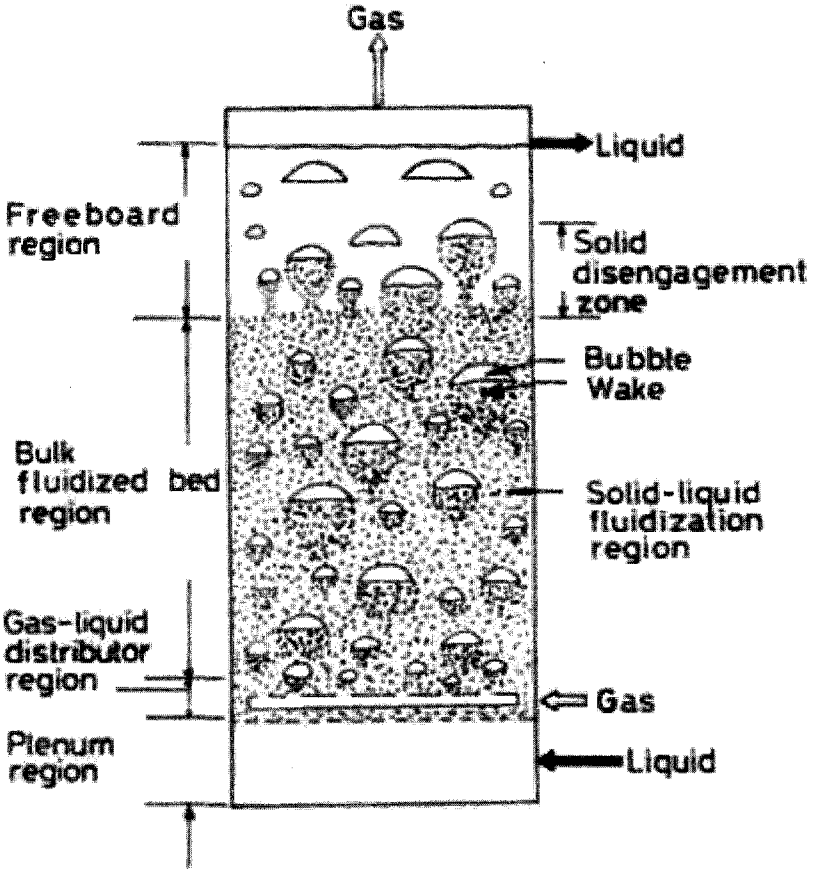

Figure 1.1: Schematic of Co-current Three-Phase Fluidized Bed (Fan, 1989)

There has been a significant amount of research on the hydrodynamics and heat and mass transfer properties of three-phase fluidized beds under ambient operating conditions using air, water and glass beads (Wild and Poncin, 1996). Industrial reactors however, are not normally operated at such conditions. They are operated at elevated temperature and pressure with complex multi-component liquids. Most research done on high pressure multiphase reactors has been done in slurry bubble columns where the particle diameter is much smaller (μm range) than for three-phase fluidized beds (mm range). For this thesis, the upgrading of petroleum resids in three-phase fluidized beds is of particular interest.

1.1 Bitumen Upgrading

Located in north eastern Alberta, approximately 440 km north of Edmonton, the Athabasca Oil Sand Deposit is the largest petroleum resource in the world (Athabasca RIWG, 2001). With an estimated 1.7 trillion barrels of bitumen, 315 billion barrels of which are ultimately recoverable with advancing technology, the Alberta Oil Sands are estimated to be able to satisfy North America's oil demand for several generations (Athabasca RIWG, 2005). The oil sand consists of sand, bitumen, mineral rich clay and water. In its raw state, bitumen is a black, highly viscous, tar-like liquid which requires upgrading for both transportation and conventional oil refining.

The Syncrude project is a joint venture consisting of eight companies operated by Syncrude Canada Ltd. Operations include mining, extraction, and upgrading at the Mildred Lake Plant and mining, primary extraction and slurry transportation at the larger Aurora Plant. The final product of the bitumen upgrading, called Syncrude Sweet Blend (SSB), is a light crude oil (30° to 32° API) with a low sulphur content (0.1 to 0.2 wt%). The result is cleaner burning oil than conventional crude oil, with no residue. In 2004, daily production of SSB averaged 238,000 barrels. Each barrel was produced at CND $18.61 and sold at a cost of CND $52.36 per barrel (Syncrude, 2005). Ongoing expansion has envisioned daily production to peak at 500,000 barrels by 2015 (Syncrude, 2005).

For this thesis, the unit of interest is the LC-Finer. The "LC" in LC-Finer stands for "Lummus and Cities Service", which are the companies involved in licensing the technology. The LC-Finer unit operates as a co-current three-phase fluidized bed, as shown in Figure 1.2. The bed in the reactor consists of cylindrical catalyst particles which become fluidized by the upward flow of separately heated hydrogen and fresh bitumen, as well as recycled internal liquid. After the gas-liquid mixture exits the bed, a recycle pan is used to disengage the gas from the liquid, and recycle the liquid to the reactor. The flow of liquid and the catalyst bed expansion is controlled by a recycle pump. The bed height is monitored via four gamma ray density detectors: two in the bed and two in the freeboard (McKnight *et al.*, 2003). Online catalyst addition and removal can be carried out. The LC-Finer unit operates at both high temperature (~440°C) and pressure (~11.7 MPa) (McKnight *et al.*, 2003).

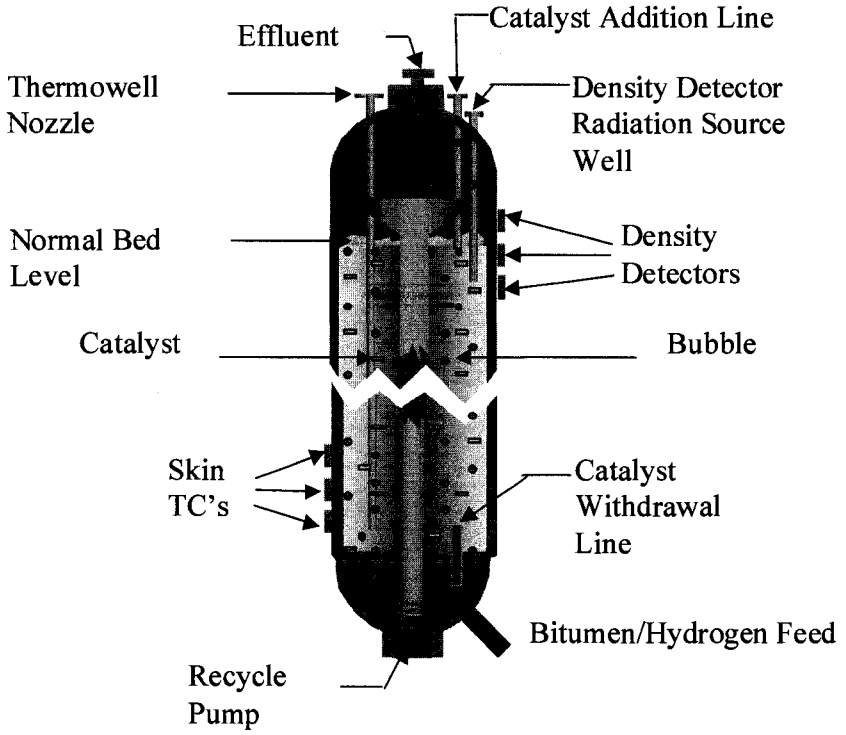

Figure 1.2: Schematic of Syncrude's LC-Finer (Macchi, 2002)

As for most industrial processes, an optimal operating condition is required. For a better understanding of a system, a model may be developed to see how changes to the system affect performance. Some of these changes may occur without warning and operators

may not be able to control the effects. One area of concern for these reactors is the re-entrainment of gas in the liquid recycle stream due to poor gas-liquid separation in the gas disengagement section. A considerable amount of gas entrained in the liquid recycle stream will significantly reduce the liquid holdup in the three-phase fluidized bed. The wear and tear on industrial components due to increased operation reduces efficiency of the components. For the gas distributor, the poor efficiency may be due to a blockage in the distributor, creating a maldistribution of the gas. The quality of bitumen sent into the LC-Finer varies. Bitumen with a greater composition of large hydrocarbons (i.e. a more viscous liquid) may have a longer residence time in the three-phase fluidized bed, therefore affecting the phase holdups. Wild and Poncin (1996) consider that an increase in liquid viscosity will increase the liquid phase holdup. An increase in the liquid phase holdup results in a decrease in the linear liquid velocity through a column, and in turn, increases the liquid residence time.

1.2 Modeling of Three-Phase Reactor Hydrodynamics

Behkish *et al.* (2006) developed a single correlation for the gas holdup in bubble columns and slurry bubble columns with a particle diameter limit of 300 x 10^{-6} m. The correlation was developed with 3881 data points retrieved from laboratory experiments and literature references. They accounted for the impact of the operating variables, reactor size, gas distributor configuration, as well as gas, liquid, and solid physical properties.

For three-phase fluidized beds, Larachi *et al.* (2001) combined neural network computing and dimensional analysis to derive correlations for the gas, solid, and liquid holdups. The data bank used to develop these correlations includes 23,000 measurements taken from about 80 references over the last four decades.

Jin (2006), and previously Liu *et al.* (2001), used the energy minimizing multi-scale (EMMS) method to characterize three-phase fluidized beds. The EMMS method is concerned with the resolution of a system into subsystems, the interaction between the phases and the energy dissipation. Both Jin (2006) and Liu *et al.* (2001) resolve a three-

phase fluidized system into the following subsystems: liquid-solid system, gas system, bubble wake system, interaction of bubble and liquid-solid system, and interaction of the primary bubble wake and the liquid-solid system. Ruiz *et al.* (2004) use the generalized wake model of Bhatia and Epstein (1974) to model the phase holdups of a high pressure three-phase fluidized bed. A common aspect between these models is the assumption that the bubble wake has a significant effect on the phase holdups of the high pressure system. A wake is produced when the bubble is large and displays a spherical cap shape. The wake is assumed to render the bubble spherical. However, under high pressure, the maximum stable bubble size is reduced, resulting in smaller spherical or ellipsoidal shaped bubbles and a more narrow bubble size distribution (Fan and Yang, 2003).

1.3 Thesis Objectives and Outline

The following goals provide the scope for the present work:

1. Develop a dimensional similitude scaling approach and propose a model to estimate phase holdups under high pressure operation relevant to an industrial hydrocracker.
2. Evaluate the effect of pressure, liquid compositions and fluid superficial velocities on the phase holdups and flow regime transition velocities of a three-phase fluidized bed.

The thesis outline is as follows: the experimental system and measurement techniques are presented in Chapter 2, a dimensional similitude scaling approach is developed in Chapter 3, Chapter 4 investigates the effect of operating conditions on overall multiphase reactor hydrodynamics and finally conclusions and options for future research are presented in Chapter 5.

Chapter 2 – Experimental Equipment and Measurement Techniques

2.1 Multiphase Fluidization System

Figure 2.1 is a schematic of the high pressure multiphase fluidization system. The system is comprised of a stainless steel (SS316) column, with an inner diameter of 0.1 m and maximum possible expanded bed height of 1.8 m. The gas and liquid superficial velocities can be respectively varied between 0.02 and 0.4 m/s and 0.01 and 0.1 m/s for pressures up to 10 MPa. Glass viewing windows, of dimensions 118.75 mm x 15.625 mm, are located at heights of 244 mm, 603 mm, and 956 mm above the top of the distributor plate allowing direct visualization. Required instruments (e.g. heat transfer probe, dissolved oxygen probe, pressure transducers) for hydrodynamic characterization can be installed at various heights and radial positions through ports located along the side, as well as the top of the column. National Instruments hardware and software are used for data acquisition.

When the system operates as a three-phase fluidized bed, a centrifugal pump (Kontro, Model: HPGSA 1X1X5/C-A1) drives the liquid from a storage tank to the base of the column. A magnetic flow meter (Rosemount, Model: 8705PSA010C7W1N0B3Q4) measures the liquid flow rate and is controlled by a needle valve. The gas is compressed via a single stage reciprocating compressor (Hydro-Pac, Model: C01.5-10-30LX) before traveling through a shell and tube heat exchanger. Fluctuations in the gas flow are minimized by four outlet gas dampeners. The compressed gas is then sent through a secondary pipe in pipe heat exchanger. Flow through the column is regulated by both inline and by-pass needle and ball valves. Prior to gas compression, a constant gas flow rate is introduced in the gas compressor by means of inlet gas dampeners. Gas is sparged in the plenum chamber of the column via a porous pipe with openings of 10 μm in diameter. The gas-liquid mixture then flows into the bed through a perforated plate with 23 holes of 3.175 mm diameter. At the top of the column, an expanded overflow section

has been designed as the primary gas-liquid separation stage. The liquid is conveyed into a partitioned liquid storage tank for further degassing and recycled to the column. The gas passes through a gas-liquid demister pad to remove any trace amounts of liquid droplets engulfed by the gas flow, and is recycled to the inlet gas dampeners.

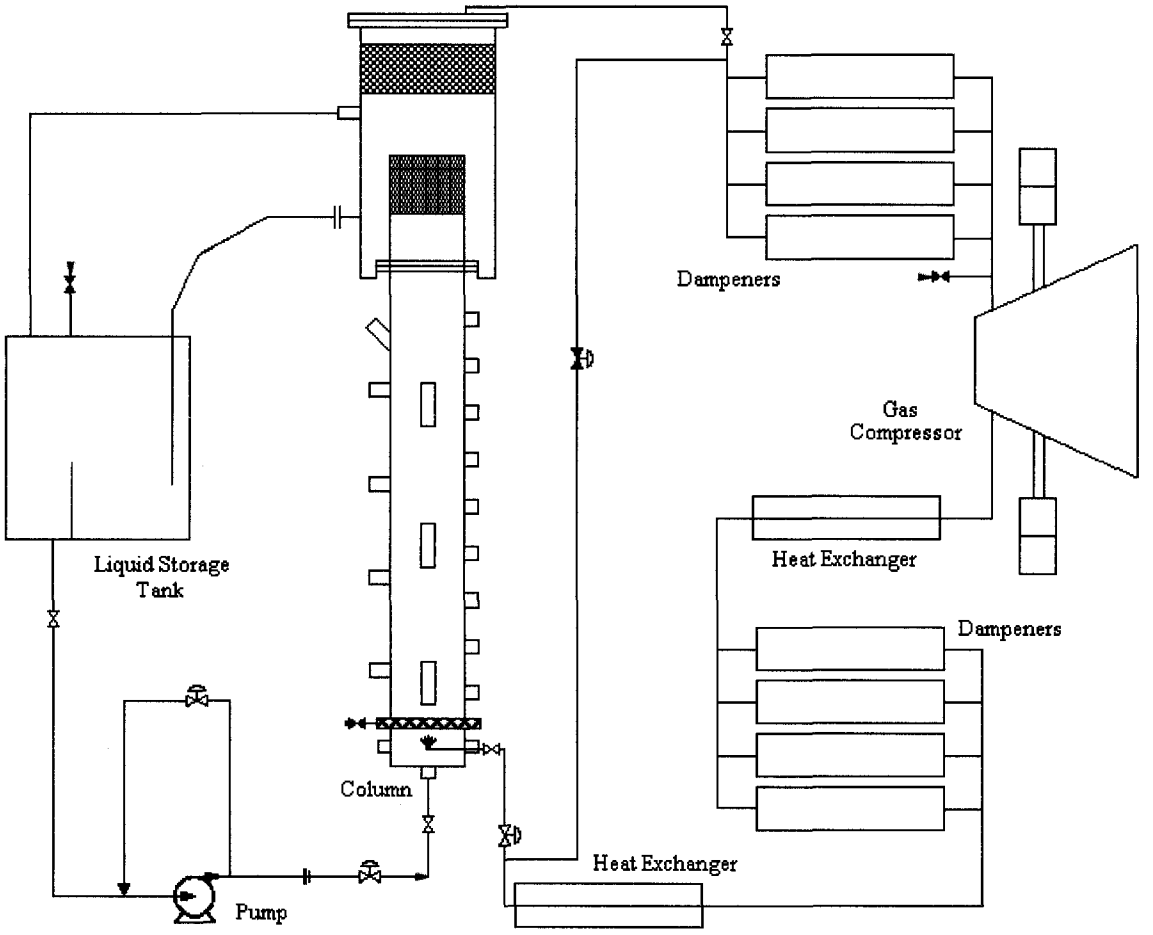

Figure 2.1: Schematic of Multiphase Fluidization Unit

2.2 General Measurement Techniques

This section describes the techniques that are used to measure the relevant hydrodynamic parameters, including the phase holdups and the minimum liquid fluidization velocity.

2.2.1 Overall Phase Holdups

Overall phase holdups are determined by measuring the dynamic pressure drops at various levels along the column. A differential pressure transmitter (Rosemount, Model: 1151DP3S22C6Q4) was used to record the pressure difference. A reference port is located at a height of 95 mm above the distributor plate. At each position, the pressure difference was recorded for 30 seconds. Figure 2.2 presents a typical pressure profile. The dynamic pressure drop ($-\Delta P$) is defined as the total pressure gradient corrected for the hydrostatic head of liquid (i.e. $-\Delta P = -\Delta P_T - g\rho_L \Delta z$).

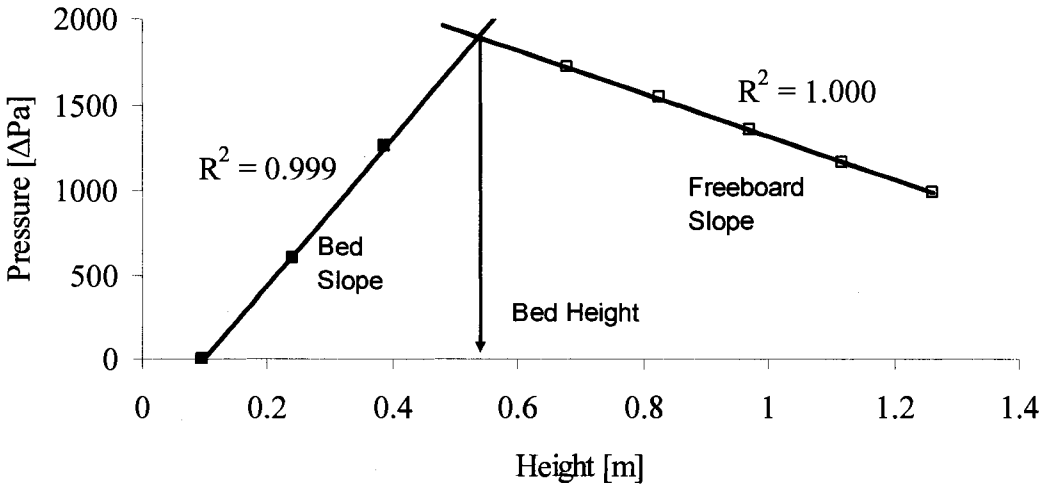

Figure 2.2: Dynamic Pressure Profile for an Air-Water-2 mm Glass Bead System for U_L = 0.071 m/s and U_G = 0.023 m/s, at a pressure of 4.5 MPa.

Bed height and bed expansion are determined from the intersection of the freeboard and bulk regions pressure gradients, which can be calculated via linear regression. The solid holdup (ε_s) can then be determined with knowledge of the bed height (H_B).

$$\varepsilon_S = \frac{4M_P}{\pi D_C^2 H_B \rho_p} \tag{2.1}$$

Where M_p is the mass of particles in the bed and ρ_p is the density of the particles. The gas holdup can be related to the pressure drop in equation 2.2 by neglecting the frictional drag on the column walls and axial acceleration of the phases.

$$\varepsilon_G = \frac{\left(\varepsilon_S(\rho_P - \rho_L) + \Delta P / g\Delta z\right)}{(\rho_L - \rho_G)} \tag{2.2}$$

The slopes of both the bed and freeboard region pressure drops are used to calculate the bed and freeboard gas holdup accordingly. Equation 2.2 is derived with the assumption that the phase holdups are independent of the height. Visual observation through the glass viewing windows verifies that an insignificant amount of particles are entrained in the freeboard region of the column as well as on the ledges of the viewing windows. The liquid holdup can then be determined with the knowledge that the sum of the phases must be unity.

$$\varepsilon_L = 1 - \varepsilon_S - \varepsilon_G \tag{2.3}$$

2.2.2 Minimum Fluidization Velocity

The minimum liquid fluidization velocity is the flow of liquid needed to suspend particles for a given gas velocity. This liquid velocity is determined from a plot of the dynamic pressure drop versus the superficial liquid velocity. In a fixed bed, the pressure drop increases with an increase in liquid velocity, while in a fluidized bed, the opposite trend is observed. A typical example is shown in Figure 2.3.

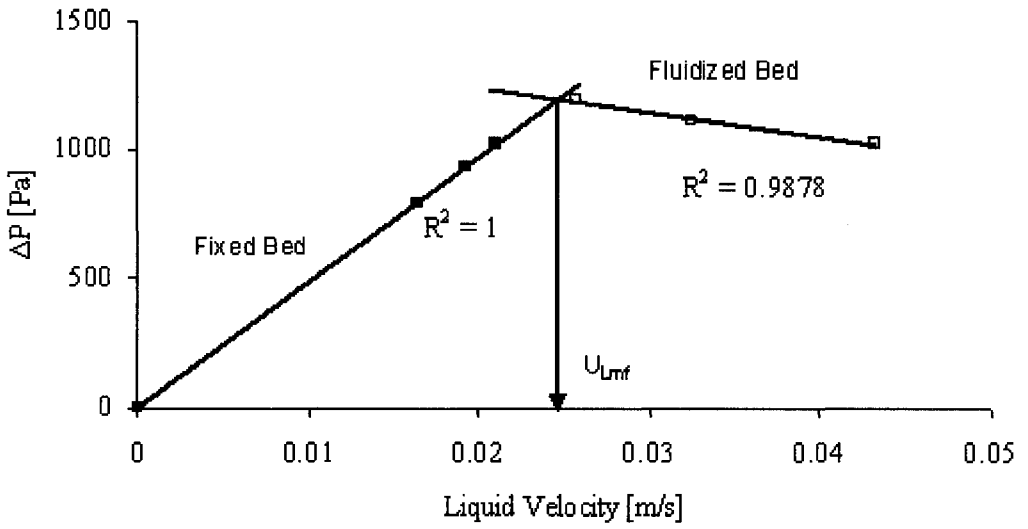

Figure 2.3: Minimum Liquid Fluidization Velocity for a Nitrogen-Water-2 mm Glass Bead System Operated at $U_G = 0$ and P = 0.1 MPa.

Chapter 3 – Dimensional Similitude Scaling Approach

Dimensional analysis and similitude is a technique in which a system can be rendered dimensionless to analyze the influence of a specific factor or property on a system. Dimensional similitude can be achieved by either using the Buckingham Pi method or by extracting the dimensionless groups of a system from the governing equations and boundary conditions. The hydrodynamics of fluidized beds can be influenced by the geometry of the equipment and the physical properties of the phases, as well as the operating conditions. Factors that can potentially influence the hydrodynamics of three-phase fluidized beds include:

- Column geometry (shape, height, internals, entrance and exit design, angle of inclination, distributors)
- Particle physical properties (size and size distribution, density and density distribution, sphericity, wettability, coefficient of restitution)
- Liquid physical properties (density, surface tension, rheology, foaming characteristics, conductivity, volatility)
- Gas physical properties (density, viscosity, solubility, diffusivity)
- Gas and liquid superficial velocities
- Bed height
- Gravitational acceleration

3.1 Buckingham Pi Method and Dimensional Similitude

The basis of the Buckingham Pi Method is to identify the variables that affect the hydrodynamics of a system. Failing to include a significant variable will lead to misleading results, while adding non-significant variables will result in extra experiments, and in the end, will be shown to be insignificant. Once the significant variables have been selected, the Buckingham Pi theorem states that for (n) dimensional variables, (n-m) independent dimensionless groups can be formed where (m) is the

number of fundamental dimensions. The results obtained from experiment describe the phenomena studied for all systems that are geometrically similar and have the same values of the dimensionless groups.

Dimensional similitude has been employed to characterize gas-solid bubbling beds (Brue and Brown, 2001), gas-solid circulating beds (Kehlenbeck *et al.*, 2001) and spouted beds (He *et al.*, 1997). Safoniuk (1999) was the first to attempt to use dimensional similitude to compare an industrial three-phase fluidized bed with a lab-scale fluidized bed. Safoniuk (1999) established eight significant independent variables that could be used to simulate the hydrodynamics of Syncrude's LC-Finer. These variables are the liquid and gas superficial velocities, liquid viscosity, liquid surface tension, liquid and particle densities, a gas-liquid buoyancy force, and the particle diameter as the characteristic length. With this list of variables, Safoniuk (1999) used the Buckingham Pi Theorem to create 5 dimensionless groups.

$$\text{M-group: } M = \frac{g(\rho_L - \rho_G)\mu_L^4}{\rho_L^2 \sigma_L^3} \qquad \text{Modified Eötvös Group: } Eo^* = \frac{g(\rho_L - \rho_G)d_P^2}{\sigma_L}$$

$$\text{Reynolds Group: } \mathrm{Re}_L = \frac{\rho_L d_P U_L}{\mu_L} \qquad \text{Density ratio: } \frac{\rho_P}{\rho_L} \qquad \text{Velocity ratio: } \frac{U_G}{U_L} \tag{3.1}$$

Larachi *et al.* (2001) also correlated solid, liquid, and gas holdups using dimensionless similitude. An exhaustive data bank consisting of 55 different liquids, 5 gases, elevated temperatures and pressure, and solid particles with various sizes, shapes and densities were used. The list of variables used by Larachi *et al.* (2001) are consistent with the variable proposed by Safoniuk (1999) with the addition of the gas density and viscosity, as a result of elevated pressure, the diameter of the column, and a bubble coalescence index. With this list of variables, Larachi *et al.* (2001) used the Buckingham Pi Theorem and created 6 dimensionless groups.

Capillary Group: $Ca_G = \frac{U_G \mu_G}{\sigma_L}$ Inertial Lockhart-Martinelli Ratio: $X_{GL} = \frac{\rho_G U_G^2}{\rho_L U_L^2}$

$$\text{Morton Group / Eötvös Group: } \frac{Mo}{Eo} = \frac{\mu_L^4}{\rho_L \sigma_L^2 d_p^2 (\rho_L - \rho_G)} \qquad (3.2)$$

Froude Group: $Fr_G = \frac{U_G^2}{g d_p}$ Wall Effect Ratio: $F = \frac{d_p}{D_C}$ Coalescence Index: 1 or 2

3.2 Selection of Influential Factors and Dimensionless Groups

Many researchers have limited the set of important characteristics in determining which variables are to be used in estimating the hydrodynamics of three-phase fluidized beds. Strict equality of the ratios of particle diameter to column diameter and column diameter to column length are deemed unnecessary if these ratios are sufficiently large that wall effects ($D_C/d_p > 30$) and entrance and exit effects ($H_B/D_C > 5$) are considered negligible. The LC-Finer at Syncrude utilizes an internal pipe for a liquid recycle stream, which is not simulated by the column at the University of Ottawa. This is not a major limitation to the dimensional similitude approach as Song *et al.* (1989) conducted experiments at high gas holdups and noticed no difference in the gas holdups between annular and non-annular systems. Catalysts used in the LC-Finer are cylindrical in shape. In lab-scale experiments, cylindrical particles are often difficult to obtain and, therefore spherical particles are used. This is not a concern as particle shape has little effect on the gas holdup as long as the particle Sauter-mean diameter is maintained (Sinha *et al.*, 1986; Song *et al.*, 1989).

Selected liquid and solid phase physical properties are similar to those proposed by Safoniuk (1999) with the exception of surface tension since the surface tension of a pure liquid does not significantly affect hydrodynamics (Gorowara and Fan, 1990). Bach and Pilhofer (1978) observed no effect of surface tension on the gas holdup for pure liquids in a bubble column, but highlighted a different behaviour for liquid mixtures. Experiments by Dargar (2005) also resulted in conclusions that the equilibrium surface tension of a

liquid was not an important characteristic of bubble columns and three-phase fluidized beds. The result shown in Figure 3.1 depicts both equilibrium and dynamic surface tension values for various liquids. The equilibrium surface tension was measured by the Wilhelmy plate method while the dynamic surface tension by the maximum pressure bubble method. By adding small amounts of surface active agents to tap water, Dargar (2005) was able to change the surface tension values without significantly changing the other physical properties of the liquid. These liquids all show a variance in equilibrium surface tensions and dilatational elasticity.

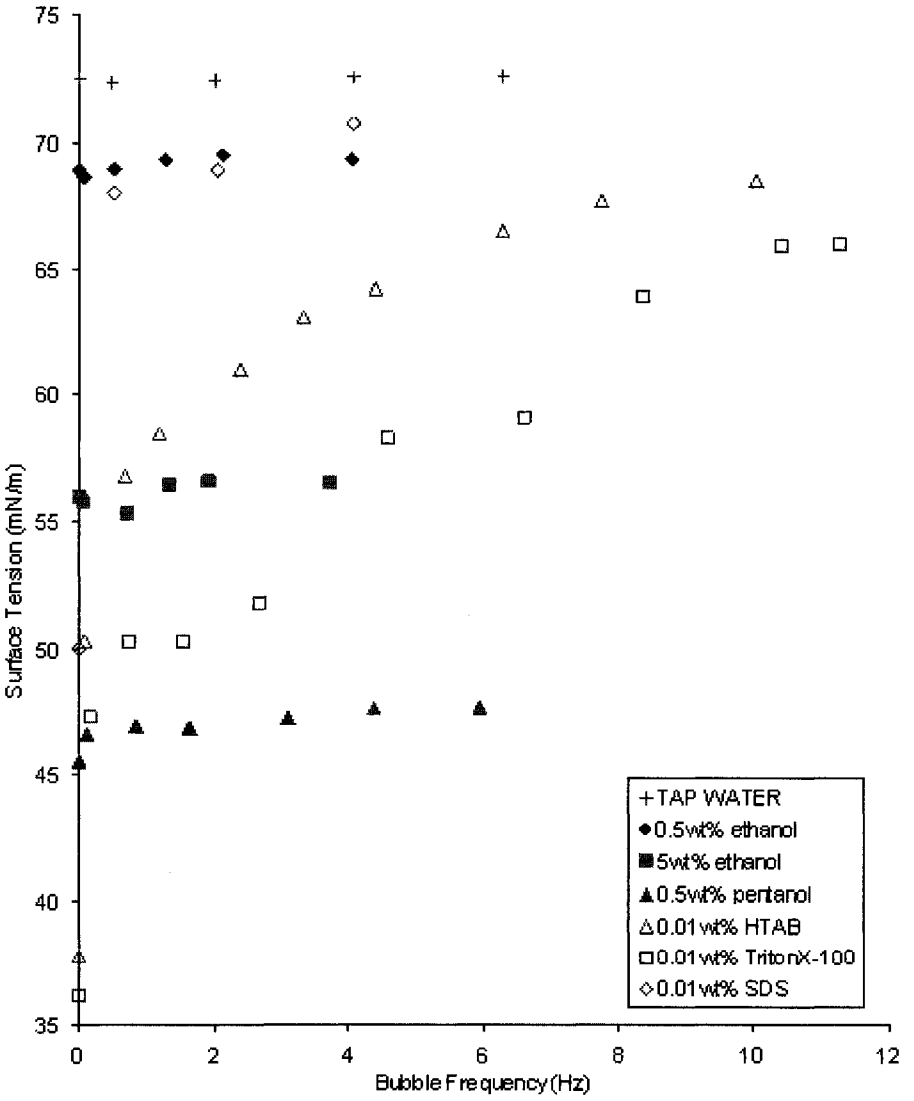

Figure 3.1: Equilibrium and Dynamic Surface Tension of Aqueous Solutions (Dargar, 2005)

Figure 3.2 shows gas holdups measured in a bubble column using the liquids presented in Figure 3.1. The surfactant solutions result in small deviations in the gas holdups, which can be grouped within +/-15%. The results show that once the concentration of surfactant in the liquid is sufficient to establish bubble coalescence inhibition, the resulting gas holdups will be similar regardless of the equilibrium surface tension value. The main difference that arises from the various surfactants is the stability of the foam head developed at a free (static) surface.

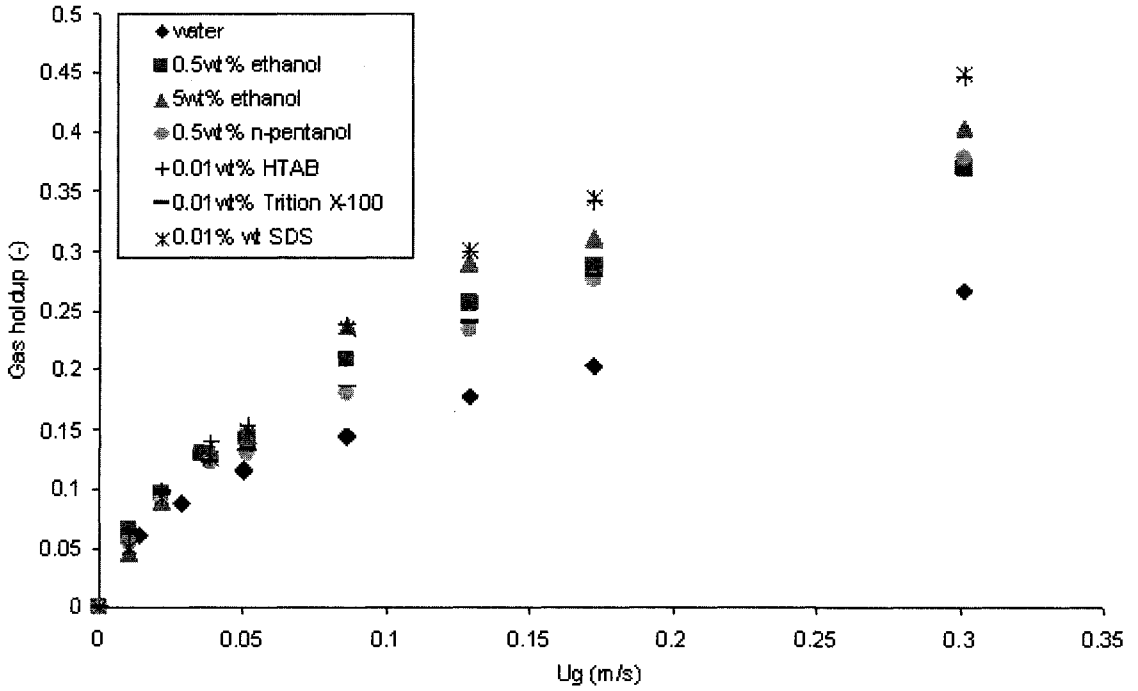

Figure 3.2: Effect of Liquid Surface Tension on Gas Holdup in Bubble Column (Dargar, 2005)

Safoniuk (1999) considered gas density an unimportant characteristic when trying to simulate three-phase fluidized beds. Macchi (2002) conducted experiments in which changes to the gas density resulted in a significant increase of the gas holdup, as shown in Figure 3.3. Changes in the gas viscosity between the systems are insignificant relative to changes in the gas density; helium (ρ_G = 0.166 kg/m^3) to sulphur hexafluoride (SF_6, ρ_G = 6.073 kg/m^3).

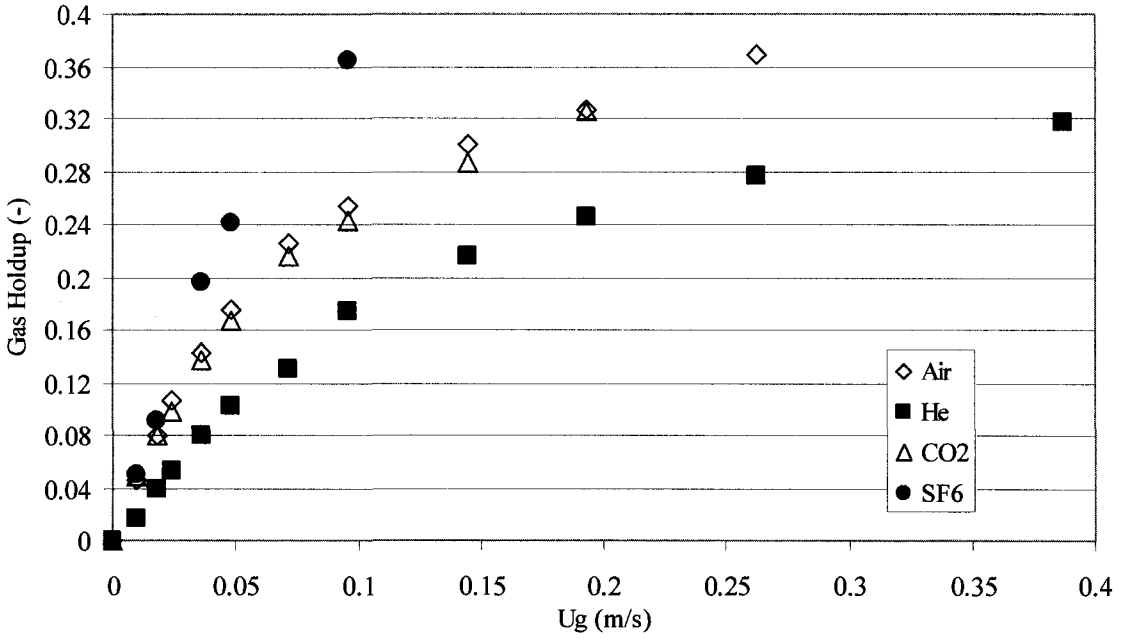

Figure 3.3: Effect of Gas Density on Gas Holdups in Bubble Column with Water/Glycerol Solution (Macchi, 2002)

Bubble coalescence inhibition can be simulated by adding minute quantities of surfactant. In small amounts, surfactants change the ability of bubbles to coalesce without significantly changing the other liquid physical properties that affect the hydrodynamics of a three-phase system. Gas density, as well as the gas-liquid buoyancy force will also be included. The last variables to be included are gas and liquid superficial velocities, as well as the bubble diameter, which is the characteristic length. There are three fundamental dimensions used in the set of variables: mass, length, and time. By applying the Buckingham Pi Theorem, five independent dimensionless groups are chosen.

$$\text{Reynolds Number: } \mathrm{Re}_L = \frac{d_B \rho_L U_L}{\mu_L} \qquad \text{Archimedes Number: } Ar_B = \frac{\rho_L g d_B^3}{\mu_L^2}(\rho_L - \rho_G) \tag{3.3}$$

$$\text{Gas-Liquid Density Ratio: } \frac{\rho_G}{\rho_L} \quad \text{Particle-Liquid Density Ratio: } \frac{\rho_P}{\rho_L} \quad \text{Velocity Ratio: } \frac{U_G}{U_L}$$

It is however difficult to estimate the bubble diameter via the operating conditions. Just as the gas holdup is a function of the above dimensionless groups, the ratio of particle to bubble diameter is a function of the same dimensionless groups. Therefore, if the ratio of

d_p/d_B is equivalent for two systems, then the values of the dimensionless groups of the two systems must be equal and the particle diameter can be inserted in place of the bubble diameter. The resulting dimensionless groups are:

$$\text{Reynolds Number: } \mathrm{Re}_L = \frac{d_P \rho_L U_L}{\mu_L} \qquad \text{Archimedes Number: } Ar_p = \frac{\rho_L g d_P^3}{\mu_L^2}(\rho_L - \rho_G) \tag{3.4}$$

$$\text{Gas-Liquid Density Ratio: } \frac{\rho_G}{\rho_L} \quad \text{Particle-Liquid Density Ratio: } \frac{\rho_P}{\rho_L} \quad \text{Velocity Ratio: } \frac{U_G}{U_L}$$

3.3 Dimensionless Comparison of Laboratory and Commercial Reactors

The aforementioned set of dimensionless groups will be used to simulate the LC-Finer hydrodynamics. Nitrogen gas, 2mm glass beads, and water, with and without small amounts of surfactant are selected to be used at the University of Ottawa. The surfactant solution will be a 0.5% weight aqueous ethanol solution as it inhibited bubble coalescence and produced an effervescent foam head at a free surface (Dargar, 2005). A comparison of the dimensionless groups that were matched is shown in Table 3.1.

***Table 3.1**: Comparison of Dimensionless Groups of the University of Ottawa High Pressure Column relative to Syncrude's LC-Finer*

Dimensionless Group	Ratio of dimensionless groups
$\pi_1 = U_G/U_L$	1
$\pi_2 = \rho_G/\rho_L$	1
$\pi_3 = \rho_S/\rho_L$	1.03
$\pi_4 = U_L d_p \rho_L/\mu_L$	0.97
$\pi_5 = \rho_L g \Delta\rho d_p^3/\mu_L^2$	0.93

Chapter 4 – Results and Discussions

The following chapter presents the experimental results and discussion regarding the hydrodynamics of liquid-solid, gas-liquid and gas-liquid-solid fluidized beds.

4.1 Liquid-Solid Fluidized Bed Hydrodynamics

The effect of pressure and/or the presence of surfactants on the phase holdups of a liquid-solid fluidized bed were evaluated. Solid holdups were determined using the dynamic pressure drop across the bed. Repeat experiments were not performed for the liquid-solid system as the slopes in the bed resulted in a minimum R^2 value of 0.99.

Figure 4.1 presents the liquid holdup as a function of liquid superficial velocity for water and the 0.5%wt aqueous ethanol solution at various pressures. Bed expansions for all four systems were relatively similar. Phase holdups are thus not significantly affected by the relatively small change in physical properties of the liquid.

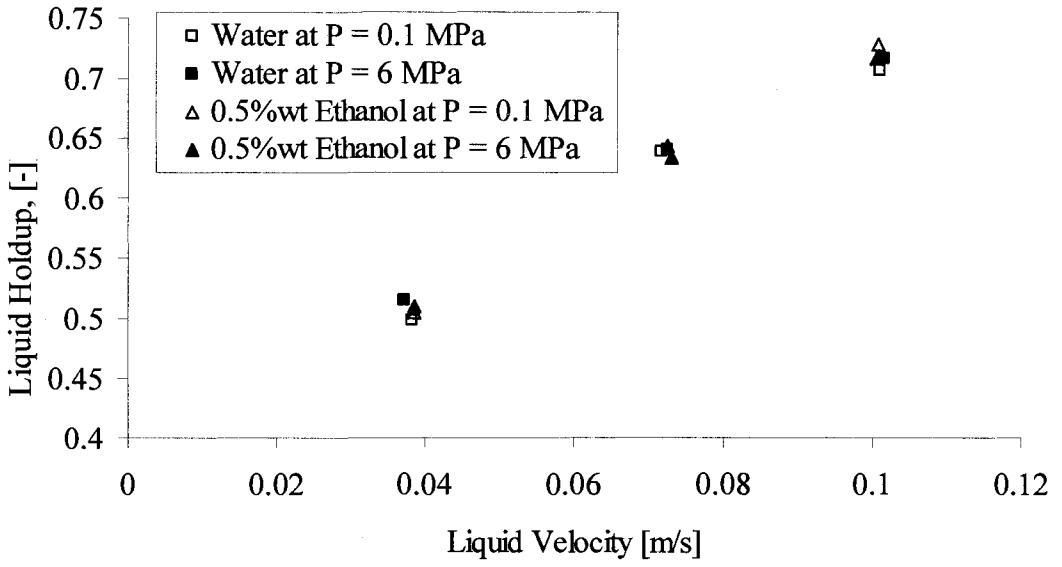

Figure 4.1: Liquid Phase Holdups versus U_L for water and 0.5%wt Ethanol Solution at Various Pressures in a Liquid-Solid Fluidized Bed

Phase holdups in the water and 0.5%wt ethanol systems are correlated via the equation of Richardson and Zaki (1954):

$$\varepsilon_L = \left(\frac{U_L}{U_i}\right)^{1/n} \tag{4.1}$$

Where U_i is determined from the intercept at $\varepsilon_L = 1$ on a $\log(\varepsilon_L)$ vs. $\log(U_L)$ plot and n from the slope. As there is no significant effect of pressure or surface tension, values of n and U_i are 2.73 and 0.286 m/s, respectively.

The parameters of n and U_i can also be estimated by the equation of Khan and Richardson (1989), shown in equation 4.2, and from the particle terminal velocity corrected for wall effects (U_i). Equation 4.2 relates the parameter (n) to both wall effects and the Archimedes Number with limits of $0.001 < d_p/D_C < 0.2$ and $10^{-2} < Ar < 10^{10}$.

$$\frac{4.8-n}{n-2.4} = 0.043 Ar^{0.57}\left(1-1.24\left(\frac{d_p}{D_C}\right)^{0.27}\right) \tag{4.2}$$

The terminal velocity of an isolated smooth sphere (v_t) for $0.3 < Re_t < 500$ is:

$$v_t = \frac{0.153 d_p^{1.143} g^{0.714} (\rho_P - \rho_L)^{0.714}}{\rho_L^{0.286} \mu_L^{0.428}} \tag{4.3}$$

$$\log_{10}\left(\frac{v_t}{U_i}\right) = \frac{d_p}{D_C} \tag{4.4}$$

From the above correlations, n = 2.52 and U_i = 0.286 m/s with an average absolute relative error (AARE) of 7.64% and 0.25%, respectively. The AARE is defined as:

$$AARE = \frac{1}{j}\sum_{i=1}^{j} abs\left(\left(Experimental(i) - Estimated(i)\right)/Experimental(i)\right) \tag{4.5}$$

4.2 Gas-Liquid Bubble Column Hydrodynamics

The following section presents the hydrodynamics of gas-liquid bubble columns, including the phase holdups and dispersed to coalesced bubble flow transition gas velocity at various pressures using water and 0.5%wt aqueous ethanol solution. There will be an attempt to correlate the data using previously reported correlations.

4.1.2 Phase Holdups

Figure 4.2 exhibits the gas holdup in water as a function of superficial gas velocity at various pressures using both a batch and a liquid circulating system. In the batch bubble column, an increase in gas velocity leads to an increase in gas holdup. At the larger gas velocities, bubbles tend to coalesce resulting in greater bubble rise velocities, and the rate of increase in gas holdup becomes smaller. Similar trends are observed at the elevated pressures. As the pressure is increased, the gas holdup increases due to enhanced bubble break-up and a decrease in bubble coalescence (Lin *et al.*, 1998; Wilkinson *et al.*, 1990). The effect of pressure is more significant at lower than at higher pressures, as the effect eventually begins to subside. Any further increase in the pressure does not affect the gas holdup as the equilibrium bubble size cannot be reduced further by increasing pressure. The effect of pressure is also more significant at higher gas velocities. At low gas velocities, the bubbles are already close to the equilibrium bubble size, and an increase in pressure does not significantly reduce the bubble size. Similar results are seen in the work of Luo *et al.* (1999).

The transition from dispersed to coalesced bubble flow regime is a gradual phenomena, occurring over a range of gas flow rates. However, the transition velocity can be determined at the change in slope of the gas velocity versus gas holdup plot. An increase in pressure delays the onset of coalesced bubble flow and the gas holdup at the transition is larger. The transitions gas velocities are estimated as 0.04, 0.045 and 0.06 m/s at 0.1, 1, and 4.5 MPa, respectively. The gas holdups at the point of transition are estimated as 0.13, 0.18, and 0.25 at 0.1, 1, and 4.5 MPa, respectively.

In the circulating bubble column, with a liquid superficial velocity of 0.071 m/s, the trends are similar to that of the batch bubble column. The liquid flow delays the transition to coalesced bubble flow and the gas holdup is larger at the transition. The gas distributor in the column operates as a two stage distributor. Gas is first passed through the pipe sparger and then re-distributed by the perforated plate. The increased shear force exerted by the liquid flow on the bubbles at the perforated plate causes the bubbles to be initially smaller. In the water system, with no significant surface-active compounds present, the bubbles can re-coalesce after the perforated plate distributor. Due to this shear force, the effect of pressure is not as great as when U_L = 0 m/s. At higher gas velocities, the bubbles do coalesce and the effects of pressure on bubble break-up becomes more apparent. Under the operating conditions shown, the effect of pressure on the gas holdup cannot be distinguished for pressures between 1 and 4.5 MPa.

The liquid flow results in a decrease in the gas holdup for all conditions with the exception of the atmospheric pressure data. The decrease in gas holdup may be due to the greater rise velocity of the bubbles. At atmospheric pressure, the bubbles are capable of re-coalescing. The re-coalescing rate of the bubbles is not sufficient to match the bubble break-up rate from the distributor, hence the bubbles are smaller, and result in larger gas holdups.

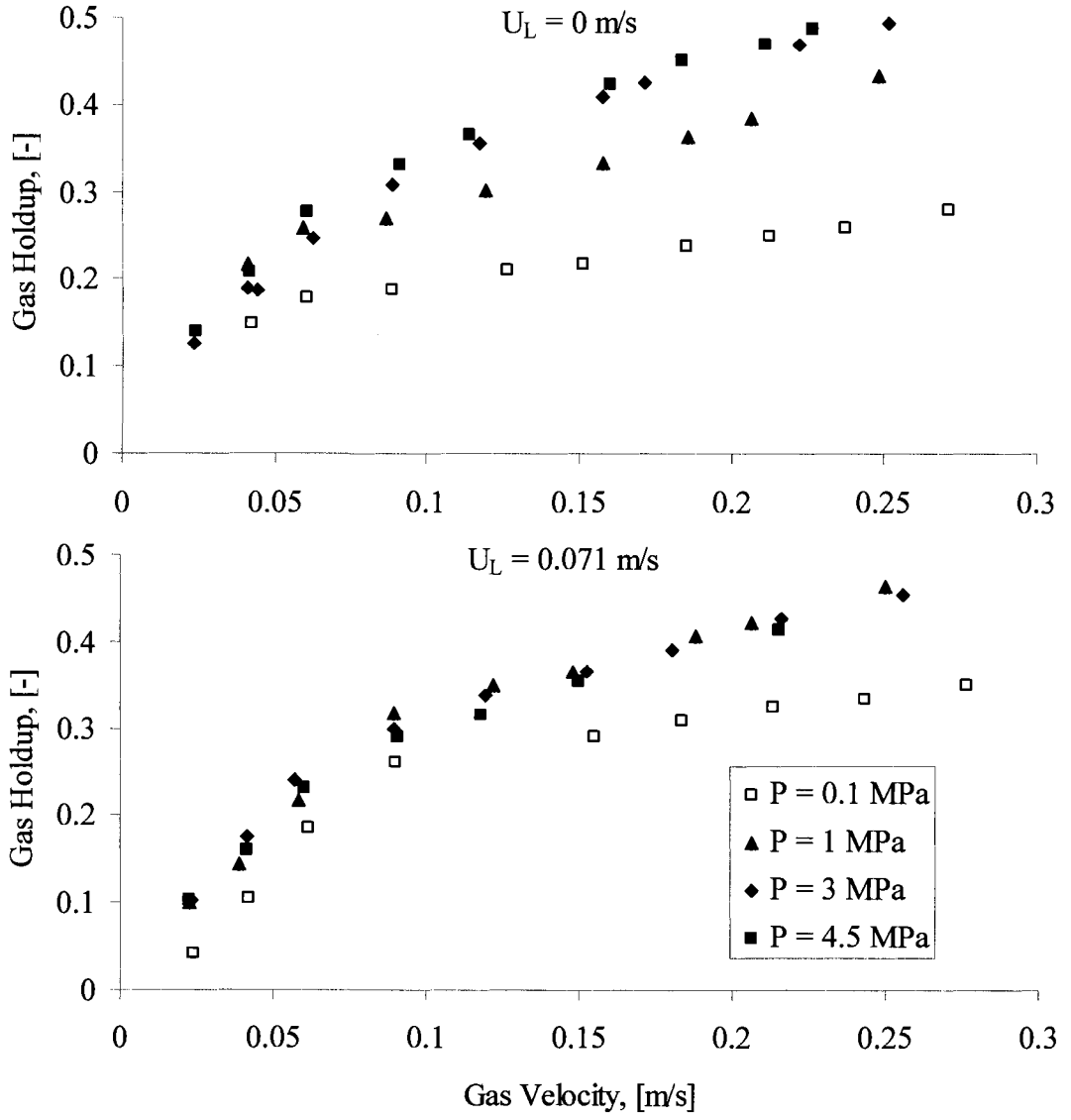

Figure 4.2: Overall Gas Holdups versus U_G for Water at Various Pressures in a Bubble Column at U_L = 0 m/s and U_L = 0.071 m/s

Figure 4.3 depicts the gas holdup for the ethanol solution at various pressures for both batch and liquid circulation. The bubbles in the ethanol solution are smaller than those in the water system. The ethanol liquid also creates a foam layer at the top of the batch bubble column. It is important to note that the data were taken in the bubbly region of the column below the foam layer. Experiments performed at elevated pressures (P = 3 and 4.5 MPa) are not shown as the increase in pressure enhances the foaming characteristics of the liquid, transitioning the foam from a stable layer above the liquid to an unstable layer which continuously grows. The foam head at these pressures

encompasses the entire column, and readings in the bubbly region can not be made. At the closure of gas flow, the foam head dissipates within seconds at all pressures. The ethanol solution becomes opaque at high gas flow rates when bubbles coalesce and yield turbulent phase mixing.

In batch operation, the trends are similar to those of tap water. The gas holdup increases with an increase in gas velocity and the gas holdup is greater at higher pressures. The addition of ethanol results in an increase in the dispersed to coalesced bubble flow transition velocity from U_G = 0.045 to 0.07 m/s at atmospheric pressure and U_G = 0.06 to 0.15 m/s at 1 MPa. Due to bubble coalescence inhibition, gas holdups in the 0.5%wt ethanol solution are greater than in the water at all pressures.

In the circulating bubble column, the column operates as a frothy mixture of gas and liquid. Once liquid flow is initiated, there is a large population of microbubbles (d_B < 1 mm). Due to the surfactant, the shear effect across the perforated plate is more pronounced and bubbles hardly coalesce in the bulk of the bed, leading to very high gas holdups, e.g. above 50%.

With a liquid velocity of U_L = 0.071 m/s, the trends are again similar to those of water. An increase in gas velocity increases the gas holdup. The dispersed to coalesced bubble flow transition velocity is again increased when a liquid flow is present. In the dispersed bubbling regime, the additional bubble coalescence inhibition due to the surfactant results in bubbles that cannot be broken down further by pressure; hence there is an insignificant effect of pressure. As the gas flow rate is increased and the column operates in the coalesced bubbling regime, the effect of pressure on bubble break-up becomes apparent. The liquid flow results in an increase in gas holdup, which is the opposite trend shown by Dargar (2005). If the distributor had no effect on the initial bubble size, then the gas holdups would be lower due to the increased rise velocity of the bubbles. The shearing effect of the distributor results in decreased bubble sizes compared to the batch system, hence the gas holdups are larger. Naturally, the gas holdups are larger for the ethanol solution than for water.

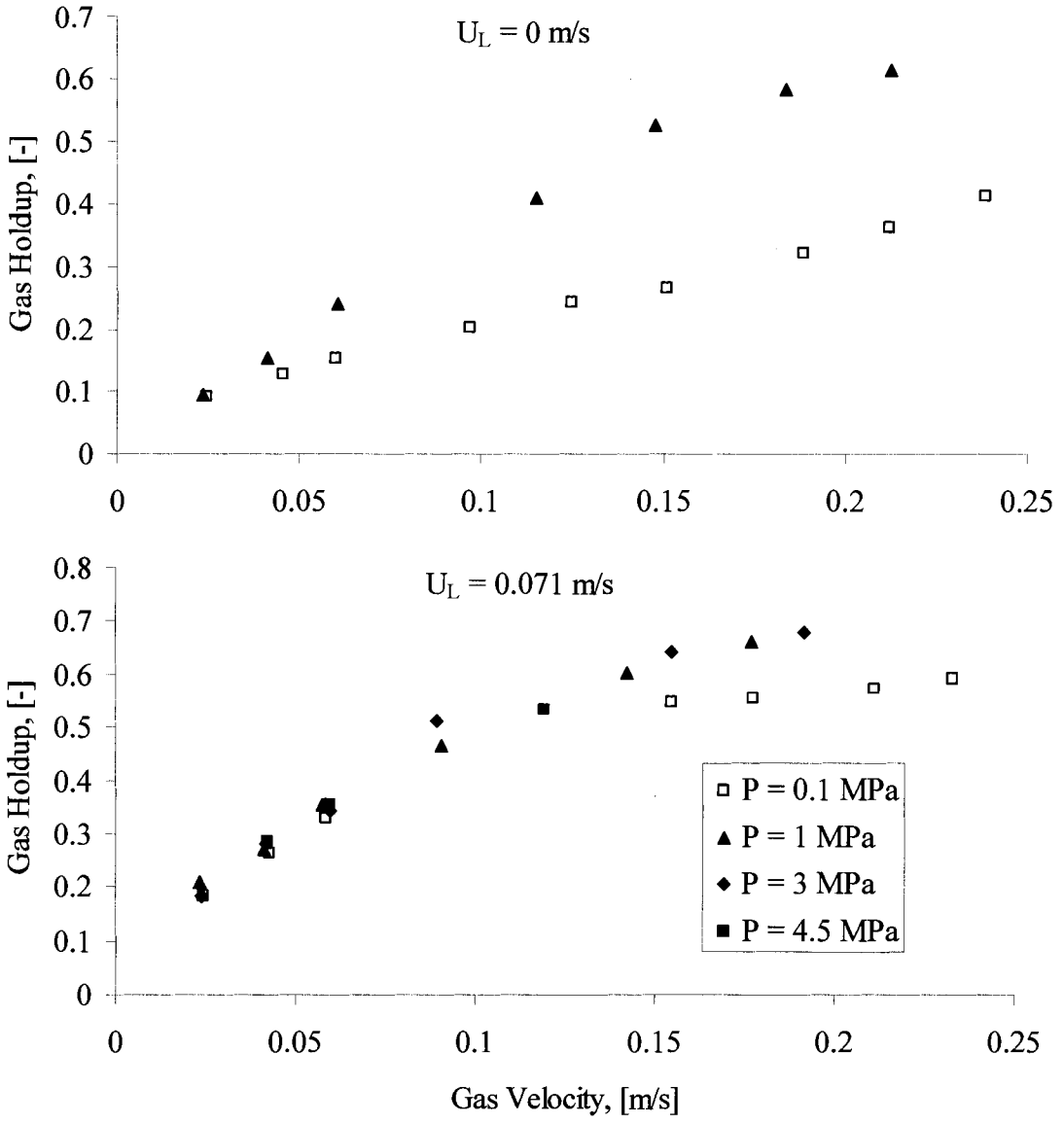

Figure 4.3: Overall Gas Holdups versus U_G for 0.5%wt Ethanol Solution at Various Pressures in a Bubble Column at U_L = 0 m/s and U_L = 0.071 m/s

4.2.2 Correlation of Gas Holdup Data

This section evaluates the performance of the gas holdup correlations of Luo *et al.* (1999) and Behkish *et al.* (2006). The correlation of Luo *et al.* (1999), shown by equation 4.6, is based on numerous gas-liquid systems operated at different operating pressures. The

correlation was developed using both mono and multi-component liquids, and the applicable ranges are outlined in Table 4.1.

$$\frac{\varepsilon_G}{1-\varepsilon_G} = \frac{2.9\left(\frac{U_G^4 \rho_G}{\sigma g}\right)^{\delta}\left(\frac{\rho_G}{\rho_L}\right)^{\beta}}{\left(\cosh\left(M^{0.054}\right)\right)^{4.1}} \quad \text{where} \quad \delta = 0.21\mathrm{M}^{0.0079} \quad \text{and} \quad \beta = 0.096\mathrm{M}^{-0.011} \qquad (4.6)$$

Table 4.1: Applicable Range of Correlation of Luo et al. (1999)

Parameters (units)	Range
ρ_L (kg/m^3)	668 – 2965
μ_L (Pa·s)	0.0003 – 0.03
σ_L (N/m)	0.019 – 0.073
ρ_G (kg/m^3)	0.2 – 90
U_G (m/s)	0.05 – 0.69
U_L (m/s)	0 (Batch)
D_C (m)	0.1 - 0.61
H_B/D_C	> 5
Distributor Types	Perforated plate, sparger, and bubble caps

The correlation of Behkish *et al.* (2006) was developed using 3881 data points obtained in bubble columns and slurry bubble columns with various pressures, temperatures, gas distributors, column diameters and particle size and densities. The correlation for bubble columns is displayed in equation 4.7, while Table 4.2 summarizes the applicable ranges.

$$\varepsilon_G = 4.94x10^{-3}\left(\frac{\rho_L^{0.415}\rho_G^{0.177}}{\mu_L^{0.174}\sigma_L^{0.27}}\right)U_G^{0.553}\left(\frac{P_T}{P_T - P_S}\right)^{0.203}\left(\frac{D_C}{D_C+1}\right)^{-0.117} x \qquad (4.7)$$
$$\Gamma^{0.053}\exp[-0.242X_W]$$

Where Γ is the effect of the distributor, P_S is the vapour pressure and X_W is the weight fraction of the primary liquid in binary liquids.

Table 4.2: Applicable Range of Correlation of Behkish et al. (2006)

Parameters (units)	Range
P (Mpa)	0.1 - 15
P_S (Mpa)	0 - 0.7
U_G (m/s)	$3.5x10^{-3}$ - 0.574
X_W	0.5 - 1.0
M_B (kg/kmol)	18 - 730
M_A (kg/kmol)	2 - 44
T (K)	275 - 538
ρ_G (kg/m^3)	0.36 - 177.3
ρ_L (kg/m^3)	633.4 - 1583
μ_L ($x10^{-3}$ Pa·s)	0.0189 - 398.8
σ ($x10^{-3}$ N/m)	8.4 - 75
D_C (m)	0.0382 - 5.5

Figures 4.4 compare the correlations of Behkish *et al.* (2006) and Luo *et al.* (1999) with the experimental data for the water and the 0.5%wt ethanol solution at pressure of 0.1 MPa and 1 MPa at a liquid flow rate of 0 m/s. The effect of concentration in the correlation of Behkish *et al.* (2006) is developed for mixtures with a significant amount of the secondary component. The small weight fraction of ethanol does not affect the correlation, and hence the predictions are similar for both the ethanol solution and water. Both correlations do an adequate job in the dispersed bubbling regime, while they overestimate the gas holdups in the coalesced bubbling regime for water and underestimate for the ethanol solution at both pressures. The overall AARE for water and the 0.5%wt ethanol solution are 21.3% and 13.9% for the correlation of Behkish *et al.* (2006) and 19.4% and 19.0% for the correlation of Luo *et al.* (1999), respectively.

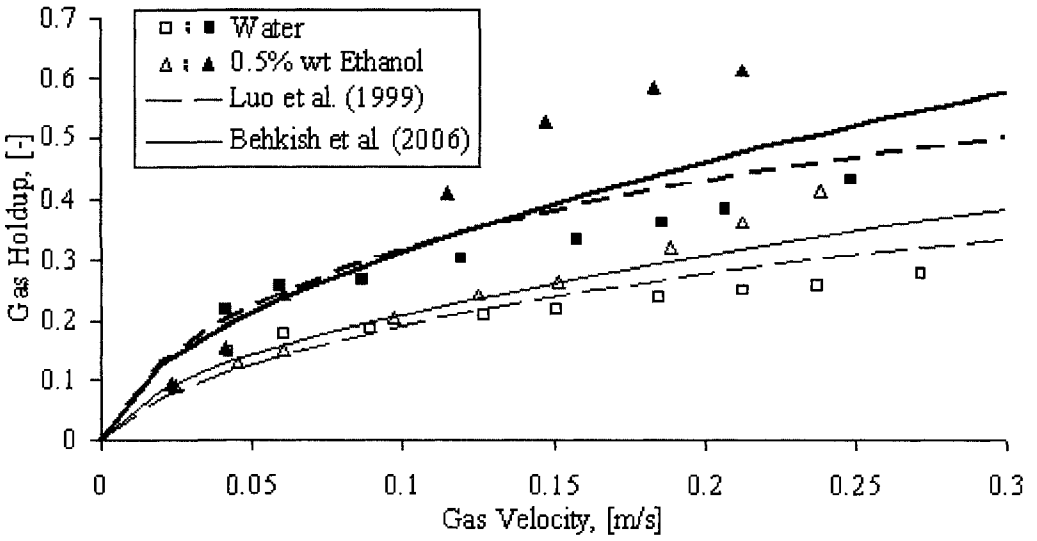

Figure 4.4: Comparison of Experimental Gas Holdups to the Correlations of Luo *et al.* (1999) and Behkish *et al.* (2006). Open and closed data points are for P = 0.1 MPa and 1 MPa, thin and thick lines are for correlations at P = 0.1 MPa and 1 MPa, respectively.

4.3 Gas-Liquid-Solid Fluidized Bed Hydrodynamics

This section describes the hydrodynamics of a three-phase fluidized bed, including the phase holdups and the minimum liquid fluidization velocity. The section will conclude with an attempt to correlate the data with previously published correlations. The first section will examine the effect of pressure on a three-phase fluidized bed using water as the liquid phase, and the second section will study the effect of pressure on a three-phase fluidized bed operating with a surfactant, 0.5%wt. aqueous ethanol solution.

In the three-phase fluidized bed using water as the liquid phase, repeat experiments have been conducted at various conditions and the average relative difference between the phase holdups is less than 5%.

4.3.1 Overall Phase Holdups for Water

Figure 4.5 displays the phase holdups as a function of the gas superficial velocities for three liquid superficial velocities using a particle diameter of 2 mm for a nitrogen-water glass bead system at atmospheric pressure. The gas holdup increases with an increase in

gas velocity for all three cases. At lower liquid flow rates, there is no significant effect of liquid velocity on the gas holdup. At the largest liquid velocity, the gas holdup is higher due to the increased shear effect of the perforated plate distributor on the gas bubbles. The effect is more pronounced at low gas velocities. Coalesced bubble flow occurs at the higher gas flow rates. The dispersed to coalesced bubble flow transition velocity is delayed with an increase in liquid velocity; from approximately 0.05 m/s at the lower two liquid velocities to 0.06 m/s at $U_L = 0.1$ m/s. The solid holdup decreases with an increase in liquid velocity and gas velocity. For all three conditions, at the introduction of gas, bubbles flowed in the dispersed flow regime and there was no bed contraction. Bed contraction is experienced only when bubble coalescence occurs at low gas velocities as the formation of large bubble removes liquid from the bed, hence increasing the solid holdup (Fan and Yang, 2003). In all three cases, the liquid holdup increased with larger liquid velocities and decreased with larger gas velocities.

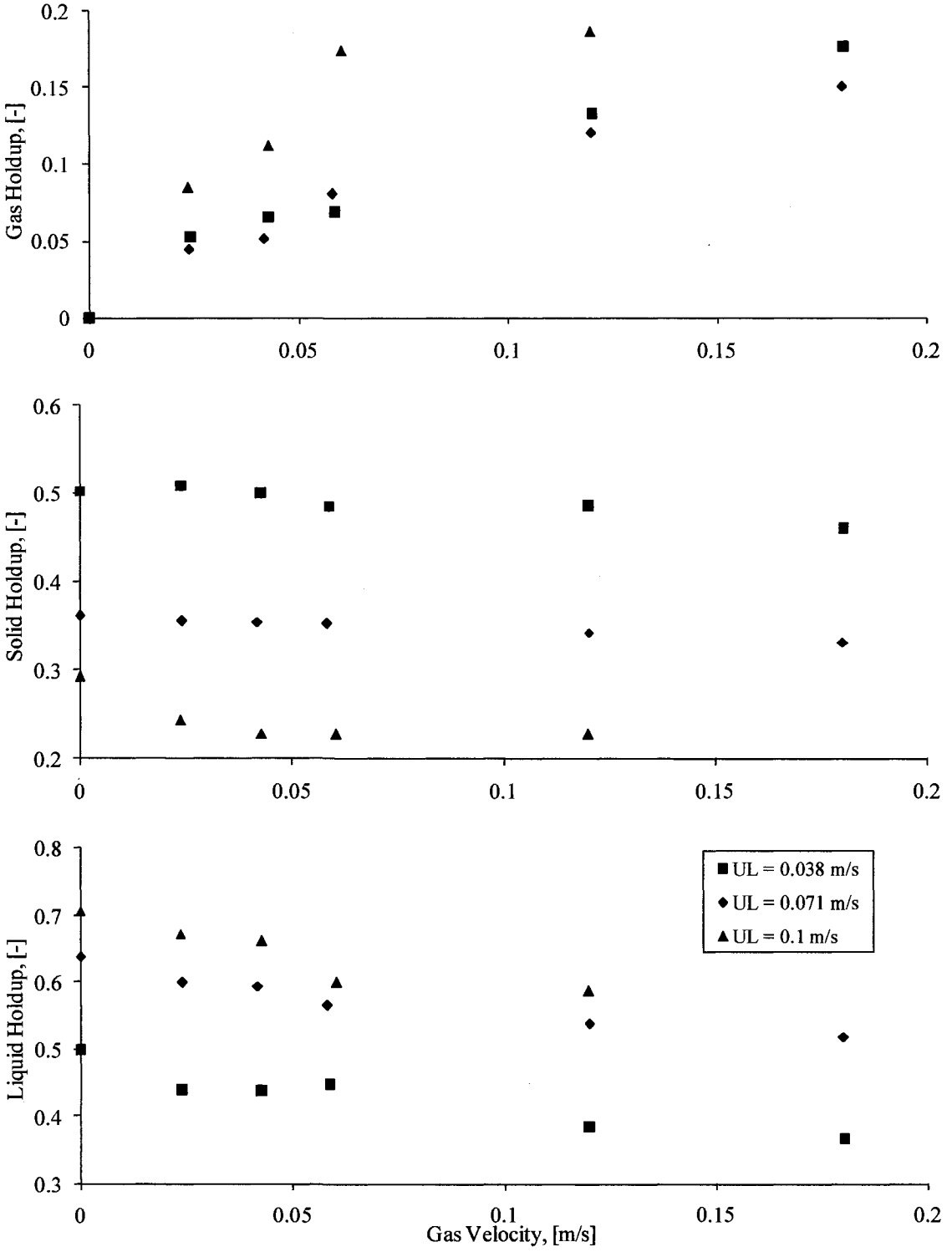

Figure 4.5: Fluidized Bed Phase Holdups for Water at 0.1 MPa using 2 mm Particles

Figure 4.6 displays the phase holdups as a function of gas superficial velocities for three liquid superficial velocities at a pressure of 4.5 MPa. The trends at elevated pressure are

similar to those at atmospheric pressure. The gas holdup is greatest at the highest liquid velocity, while the gas holdups are similar at the lower liquid velocities. The effect of liquid velocity at the lower velocities only becomes apparent at large gas velocities. The transition from dispersed to coalesced bubble flow cannot be determined at higher pressures, as the increase in pressure delays the transition to the extent where the data presented is transitioning at the largest gas velocities. Bed expansion at the introduction of gas, resulting in an initial decrease in solid holdup, is present at all conditions. The liquid holdup remains relatively constant at low gas flow rates and decreases at larger gas flow rates. At low gas velocities, the reduction in solid holdup is sufficient to counteract the increase in gas holdup. However, once the gas velocity reaches 0.04 m/s, the liquid holdup decreases considerably.

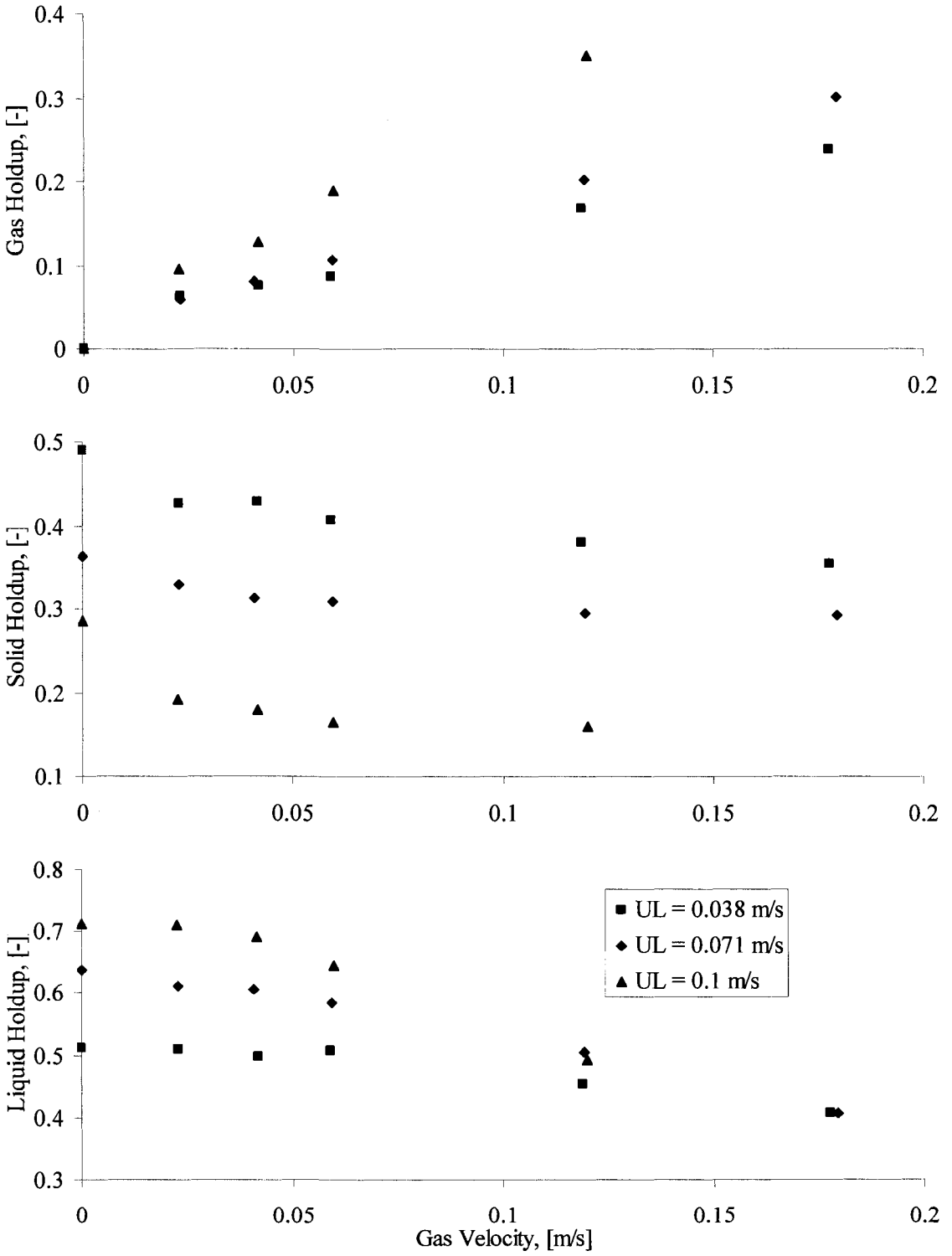

Figure 4.6: Fluidized Bed Phase Holdups for Water at 4.5 MPa using 2 mm Particles

Figure 4.7 presents the phase holdups as a function of gas superficial velocity for all of pressures examined at a liquid superficial velocity of 0.071 m/s. It can be seen that an

increase in pressure results in an increase in gas holdup. This same trend is observed in the works of Luo *et al.* (1997) and Ruiz *et al.* (2004). As with the bubble column, the effect of pressure is more pronounced at higher gas velocities where the larger bubbles can breakdown. At the lower gas velocities, the gas distribution system already produces relatively small bubbles that cannot be broken down much further. The smaller bubble sizes in high pressure three-phase fluidized beds can be attributed to smaller equilibrium bubble sizes, the suppression of bubble coalescence and the enhancement of bubble breakup (Luo *et al.*, 1997). These factors resulted in smaller, slower rising bubbles which increased the gas holdup. For these operating conditions, the gas holdups for the 4.5 and the 6 MPa systems are similar.

At the introduction of gas to all liquid-solid systems, there is a decrease in solid holdup, corresponding to an initial bed expansion. Using 1.71 mm glass beads, Ruiz *et al.* (2004) also saw a bed expansion upon injection of gas at all liquid velocities. However, Luo *et al.* (1997), using 2.1 mm glass beads and a more viscous liquid, reported a bed expansion at low liquid velocities and a bed contraction at relatively high liquid velocities at pressures up to 5.62 MPa. The results of Luo *et al.* (1997) are explained via a form of the generalized bubble wake model. However, at elevated pressures smaller equilibrium bubble sizes and enhanced bubble breakup reduce the chances of bubble wakes being present. In this work, the bed expansion is much more pronounced at elevated pressure. The liquid holdups are relatively independent of pressure at low gas velocities. However, as pressure increases at high gas velocities, the decrease in solids cannot balance the increase in gas holdup, resulting in a reduction of liquid holdup.

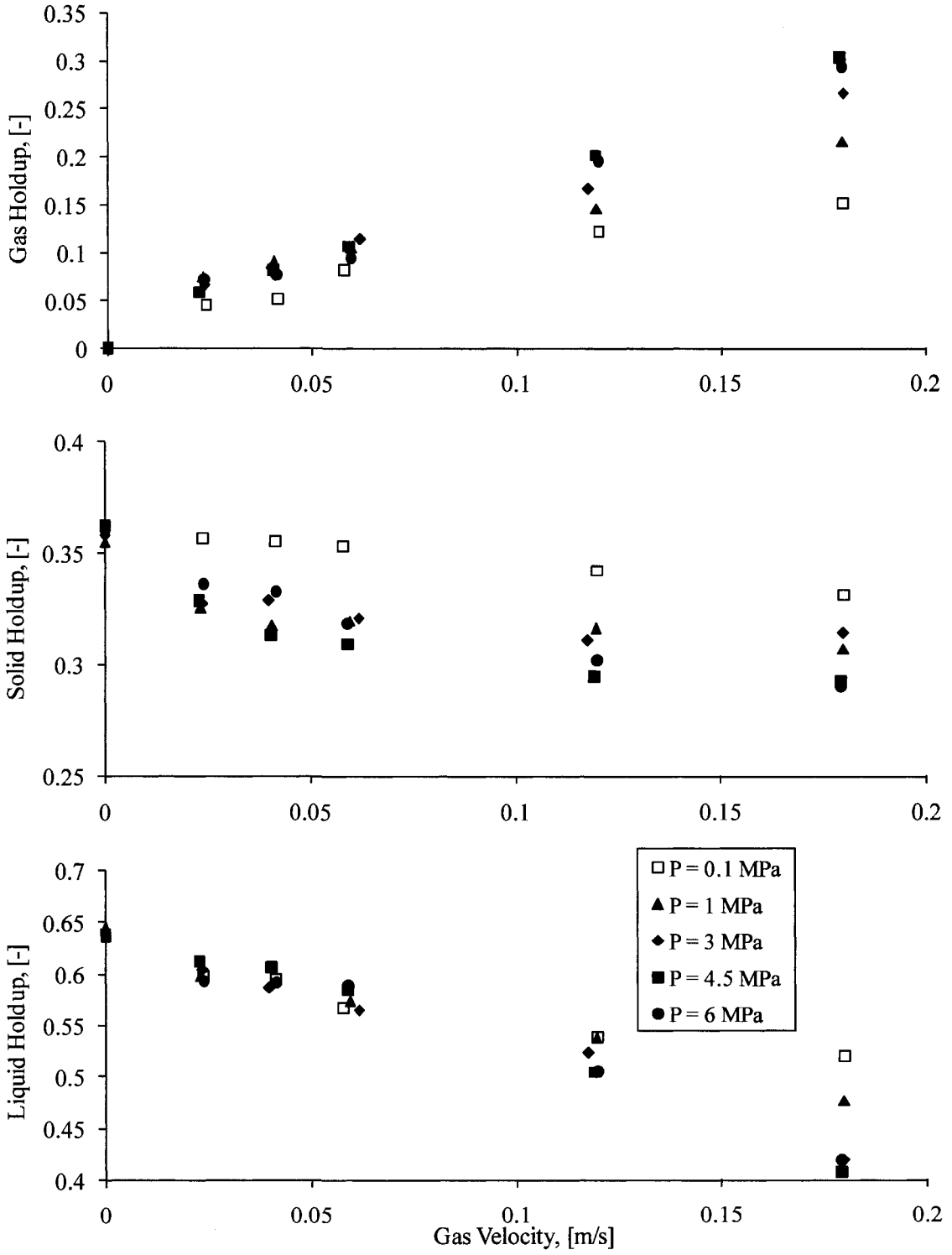

Figure 4.7: Pressure Effects on the Phase Holdups in a Three-Phase Fluidized Bed with a Water Liquid Phase at $U_L = 0.071$ m/s.

Figure 4.8 compares the gas holdups in the bed and in the freeboard region under varying pressures for water at a superficial liquid velocity of 0.071 m/s. An increase in pressure results in an increase in the gas holdup in the freeboard region. Gas holdups in the freeboard region follow the same trend as in the bed, but are always greater. At the lower gas velocities, the difference between the bed and freeboard gas holdups remains relatively constant, while this difference increases at the highest gas velocities. Gas holdups in the bed, taken on a solids-free basis, in most part underestimate the freeboard gas holdups.

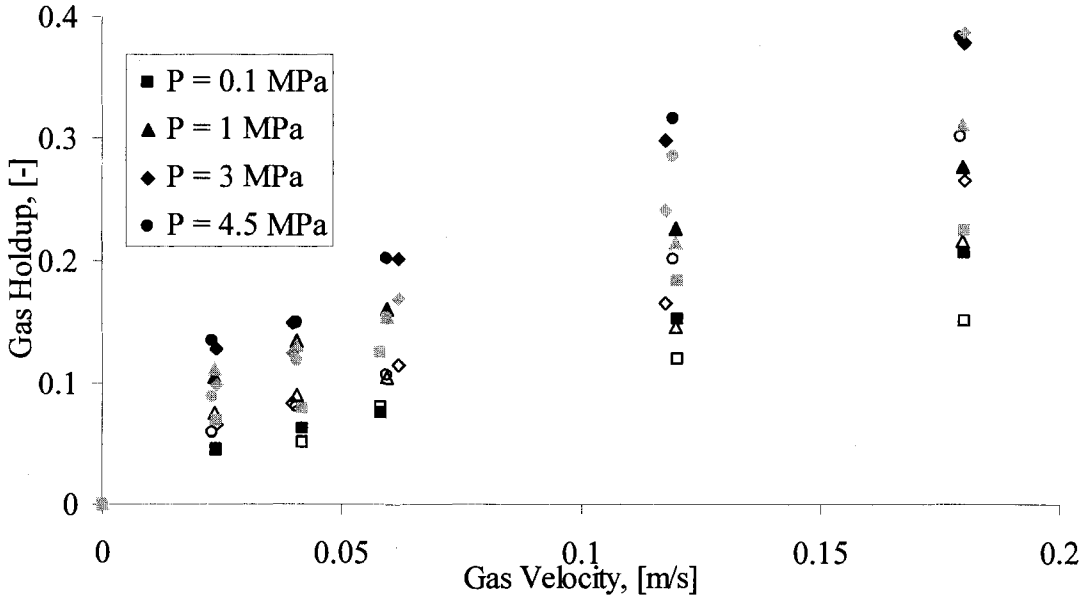

Figure 4.8: Bed, Freeboard, and Solid-Free Gas Holdups for Water at Various Pressures at U_L = 0.071 m/s. Open, black, and grey symbols represent the bed, freeboard, and solids-free gas holdup, respectively.

Figure 4.9 compares gas holdups in the freeboard of a three-phase fluidized bed to those in a bubble column for water at various pressures using U_L = 0.071 m/s. Gas holdups in the freeboard region are similar to those in the bubble column at elevated pressures. At lower pressures, bubbles exiting the bed are able to coalesce in the freeboard yielding lower gas holdups.

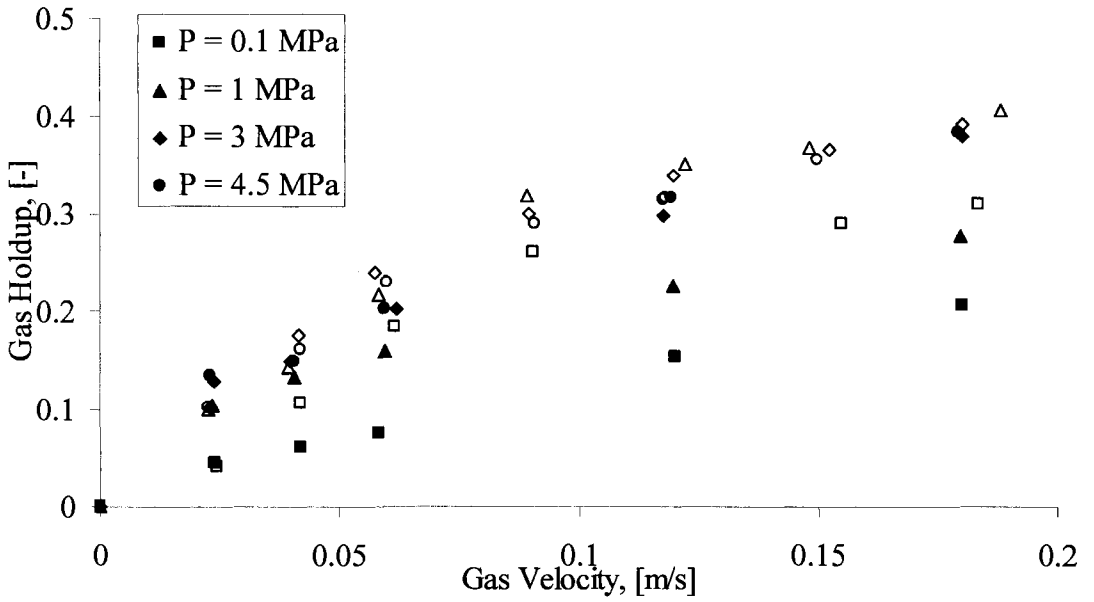

Figure 4.9: Bubble Column and Freeboard Gas Holdup for Water at Various Pressures at U_L = 0.071 m/s. Open and closed data points are for bubble column and freeboard, respectively.

4.3.2 Overall Phase Holdups for 0.5%wt Aqueous Ethanol Solution

The following section describes the effect of a surfactant on the phase holdups and compares the phase holdups to those of water. The bubbles in the 0.5%wt aqueous ethanol solution are smaller than those in water and the solution is a frothy mixture. There are many microbubbles created by the shearing at the perforated plate. The smaller bubbles lead to larger gas holdups. The foam layer at the free surface in the annulus around the top of the column is stable under atmospheric pressure, however an increase in pressure reduces the stability of the foam head.

Figure 4.10 compares the phase holdups of water and the 0.5%wt ethanol solution at atmospheric pressure at a liquid superficial velocity of 0.071 m/s. As with the bubble column, the ethanol solution yields greater gas holdups than water. Furthermore, the ethanol solution appears to still be in the dispersed bubble regime at U_G = 0.061 m/s. Data was not obtained in the coalesced bubbling regime. However, using a 1% aqueous ethanol solution with 1.2 mm glass beads at atmospheric conditions, Nacef (1991)

noticed a delay in the transition from dispersed to coalesced bubble flow as a result of the addition of ethanol to tap water. At the introduction of gas, the bed expanded due numerous small bubbles; a similar result is seen with water. At all conditions, bed expansions are significantly greater and solids holdups are lower with the ethanol solution. As the gas velocity is increased, the liquid holdup in the ethanol solution decreases substantially relative to water due to the large increase in gas holdup.

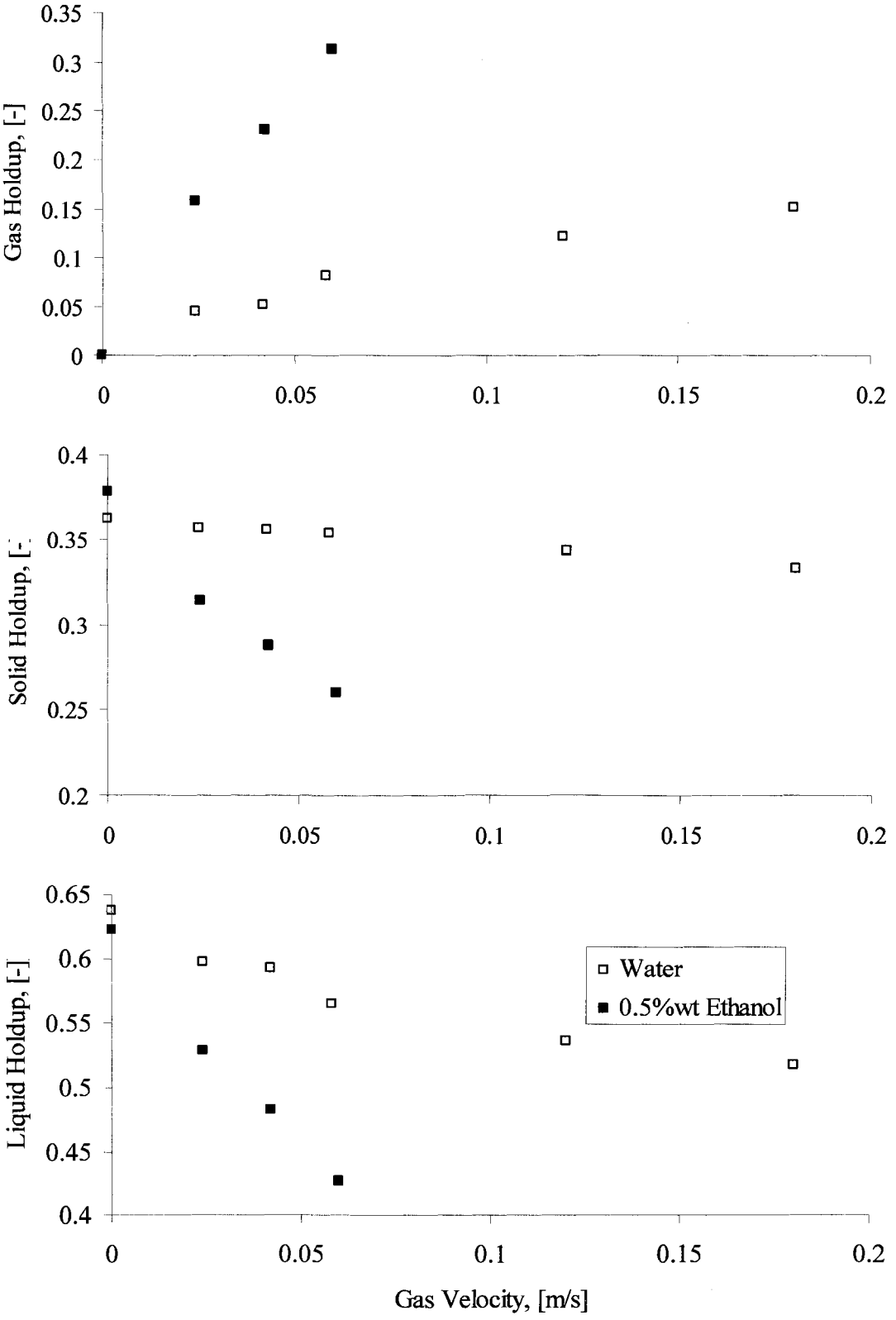

Figure 4.10: Effect of Surfactants on Phase Holdups in a Three-Phase Fluidized Bed at $U_L = 0.071$ m/s and P = 0.1 MPa

Figure 4.11 displays the phase holdups as a function of gas superficial velocity for a liquid superficial velocity of 0.071 m/s for both water and 0.5%wt ethanol solution at 4.5 MPa. Trends at elevated and atmospheric pressures are similar. The addition of ethanol results in an increase in the gas holdup. For both the water and ethanol solution, gas holdups are in the dispersed bubbling regime without a transition to the coalesced bubble flow in the data presented. The solids holdup decreases more rapidly with the ethanol solution, and the bed expansions are larger. For example, at a liquid velocity of 0.072 m/s and a gas velocity of 0.12 m/s, the bed expansion increases from 101% to 310% due to the ethanol. Again, the liquid holdups are significantly smaller for the ethanol solution.

Figure 4.12 presents the phase holdups of the 0.5%wt ethanol solution as a function of gas superficial velocity for all pressures examined at a liquid superficial velocity of 0.071 m/s. As observed in the bubble column, see Figure 4.3, there is little effect of pressure on the phase holdups over the operating range tested.

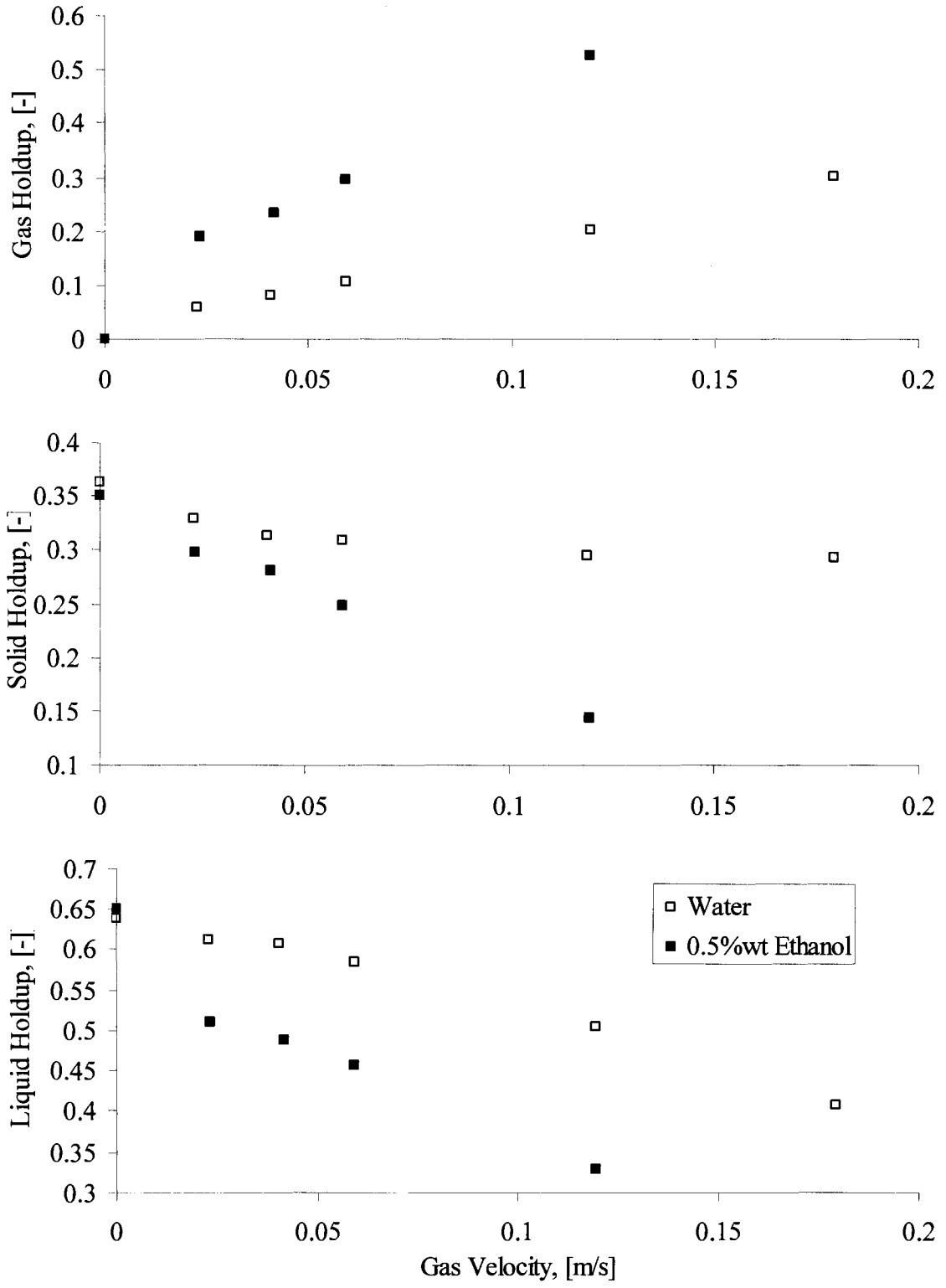

Figure 4.11: Effect of Surfactants on Phase Holdups in a Three-Phase Fluidized Bed at U_L = 0.071 m/s and P = 4.5 MPa

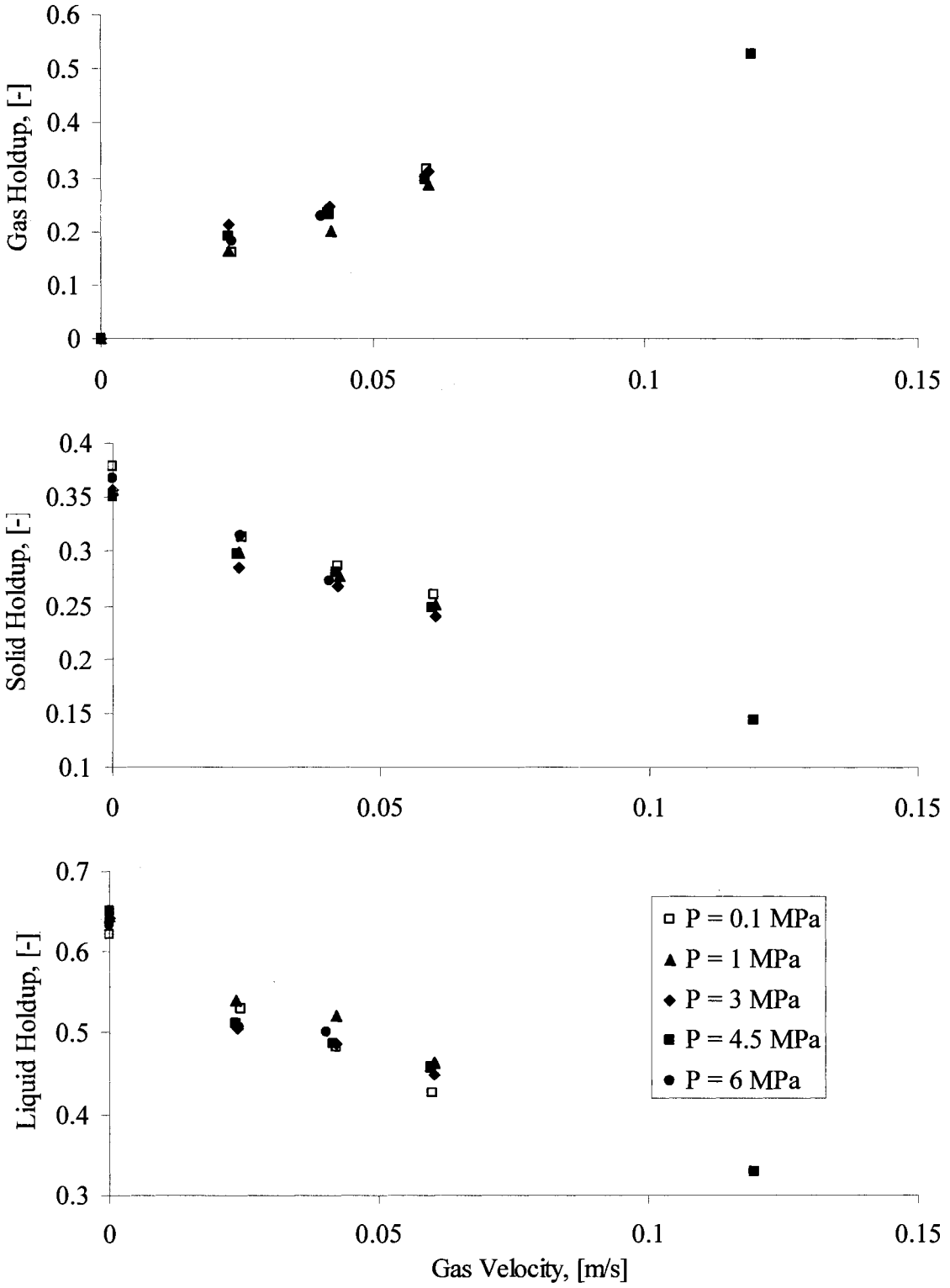

Figure 4.12: Pressure Effects on the Phase Holdups in a Surface-Active Three-Phase Fluidized Bed at $U_L = 0.071$ m/s

Figure 4.13 compares the gas holdups in the bed and in the freeboard region under various pressures for the 0.5%wt ethanol solution at a liquid superficial velocity of 0.071 m/s. Trends are similar to those observed in the water system where the freeboard gas holdup are greater than those in the bed. In this case, gas holdups in the bed, taken on a solids-free basis, represent well the freeboard gas holdups.

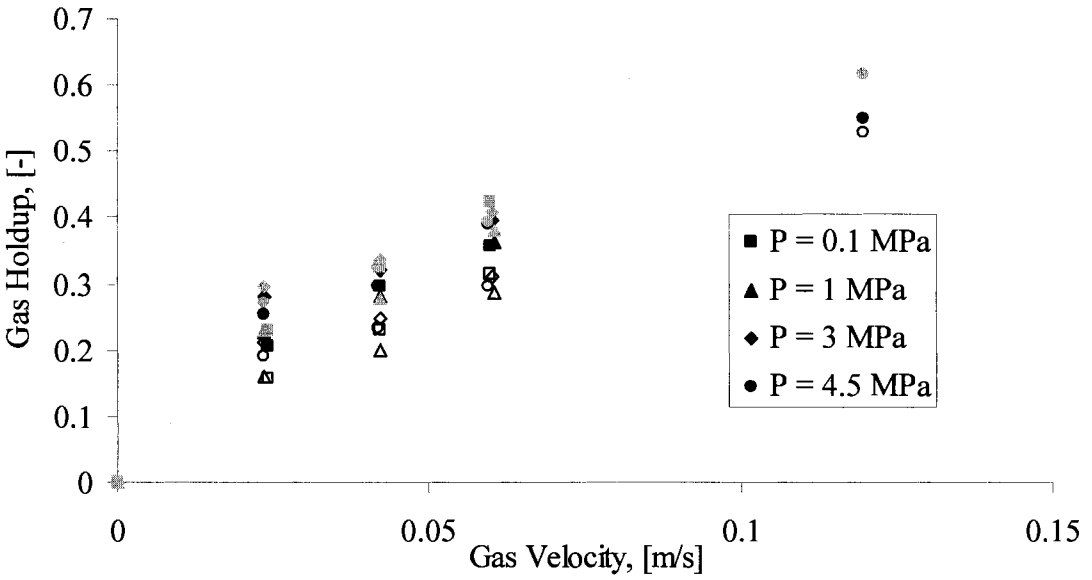

Figure 4.13: Bed, Freeboard, and Solids-Free Gas Holdups for the 0.5%wt Ethanol Solution at Various Pressures at U_L = 0.071 m/s. Open, black, and grey symbols represent the bed, freeboard, and solids-free gas holdup, respectively.

Figure 4.14 compares the gas holdups in the freeboard region to those in a circulation bubble column for a 0.5%wt ethanol solution at various pressures. Gas holdups in the freeboard region are similar to those found in a bubble column, especially at high gas velocities. This is somewhat expected as the solids holdup reduces to as low as 0.15 at the greatest gas velocities.

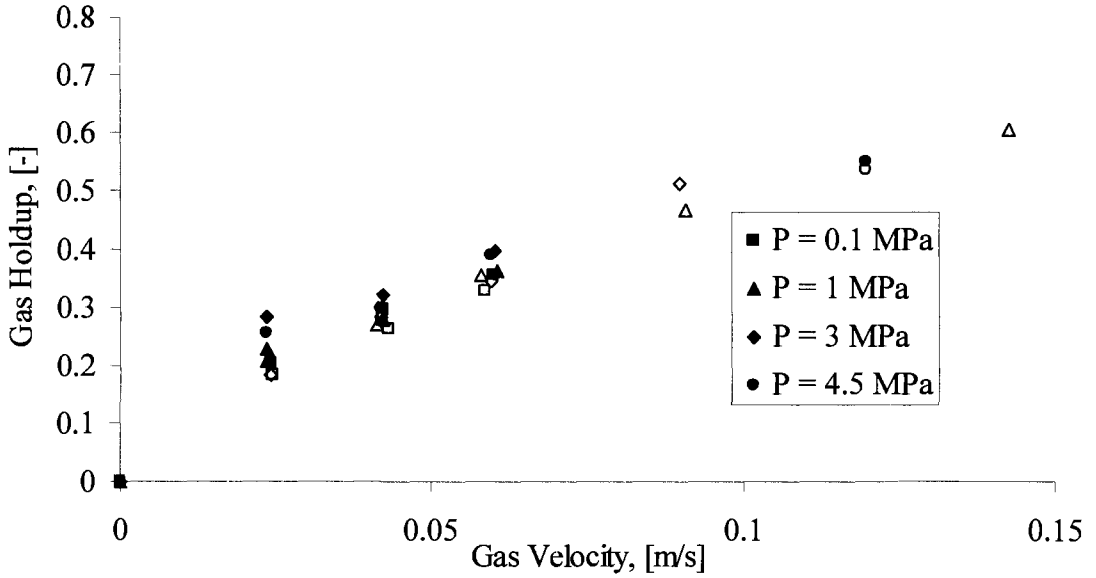

Figure 4.14: Bubble Column and Freeboard Gas Holdup for a 0.5%wt Ethanol Solution at Various Pressures at U_L = 0.071 m/s. Open and closed data points are for bubble column and freeboard, respectively.

4.3.3 Correlation of Phase Holdup Data

This section attempts to correlate the phase holdups of three-phase fluidized beds. Other than the correlation proposed by Larachi *et al.* (2001), there is no correlation for the phase holdups in three-phase fluidized beds operated at elevated pressures. The correlation of Larachi *et al.* (2001) was shown to be inaccurate (Macchi, 2002), but modification to the correlation of Han *et al.* (1990) will be examined.

Han *et al.* (1990) developed a series of correlations based on the Richardson and Zaki (1954) equation to predict the phase holdups for beds which contract or expand on initial injection of gas. The liquid holdup and solid holdup correlations were developed using 2875 and 1946 data points with an AARE of 8.7% and 6.4%, respectively. These correlations were developed at ambient temperature and pressures, and more than half of the data points were obtained using water-air-glass bead systems (Wild and Poncin, 1996). The liquid and solid holdup correlations for initial bed expansion are:

$$\varepsilon_L = \left(\frac{U_L}{U_i}\right)^{1/n}\left(1 - 0.374 Fr_G^{0.176} We_M^{-0.173}\right) \tag{4.8}$$

for $0.054 \le \frac{U_L}{U_i} \le 0.899$; $0.0000395 \le Fr_G \le 2.551$; $0.000918 \le We_M \le 5.013$

$$\varepsilon_S = 1 - \left(\frac{U_L}{U_i}\right)^{1/n}\left(1 + 0.123 Fr_G^{0.347} We_M^{0.037}\right) \tag{4.9}$$

for $0.029 \le \frac{U_L}{U_i} \le 0.481$; $0.0000173 \le Fr_G \le 3.788$; $0.00895 \le We_M \le 5.479$

Macchi (2002) modified these correlations to include the effect of pressure by the addition of the gas density. The modified correlations still reduce to the Richardson-Zaki equation at $U_G = 0$.

$$\varepsilon_L = \left(\frac{U_L}{U_i}\right)^{1/n}\left(1 - 0.374 Fr_G^{0.176} We_M^{-0.173}\left(\frac{\rho_G}{\rho_{G,STP}}\right)^{\alpha}\right) \tag{4.10}$$

$$\varepsilon_S = 1 - \left(\frac{U_L}{U_i}\right)^{1/n}\left(1 + 0.123 Fr_G^{0.347} We_M^{0.037}\left(\frac{\rho_G}{\rho_{G,STP}}\right)^{\beta}\right) \tag{4.11}$$

Based on the experimental data produced in the present work and that of Macchi (2002), the values of α and β are -0.12 and 0.03, respectively. There is an insignificant difference between the predicted water and ethanol solution gas holdups due to negligible differences in the phase physical properties. This is a false representation of the ethanol solution gas holdup as they are, for both P = 0.1 and 4.5 MPa, considerably underestimated. No further attempt is made to correlate the phase holdups of the ethanol solution via equations 4.10 and 4.11.

Table 4.3 summarizes the performance of the correlations for water at both atmospheric and elevated pressures. At atmospheric pressure, the correlation is poor for the gas holdups but adequate for liquid and solid holdups. The error on the gas holdup is a

compounded error from the solid and liquid holdup correlations, and is large due to the small gas holdup values.

Table 4.3: Modified Han et al. (1990) Correlation Performance (Eqns. 4.10 and 4.11)

Liquid	Hydrodynamic Parameter	AARE at P = 0.1 MPa	AARE at Elevated Pressures
Water	Gas Holdup	0.974	0.357
Water	Solid Holdup	0.068	0.099
Water	Liquid Holdup	0.136	0.082

The dynamic similitude approach can provide a means to develop an empirical correlation for an improved prediction of the gas holdup. Using the dimensionless groups developed in Chapter 3, along with a bubble coalescence index, a purely empirical correlation can be developed in the form:

$$\varepsilon_G = aI^b \,\mathrm{Re}^c\, Ar^d \left(\frac{U_G}{U_L}\right)^e \left(\frac{\rho_G}{\rho_L}\right)^f \left(\frac{\rho_P}{\rho_L}\right)^g \tag{4.12}$$

Where I is the bubble coalescence index (1 for mono-component liquids, 2 for multi-component liquids) and a-g are correlation parameters. Using the data obtained in this work, along with those of Nacef (1991), Macchi (2002), and Dargar (2005), multiple regression analysis determined the parameters displayed in Table 4.4. The limits of the correlation are summarized in Table 4.5.

Table 4.4: Regression Parameters of Gas Holdup Correlation (Eqn. 4.12)

Parameter	Regression Value
A	0.205
B	0.619
C	0.579
D	-0.072
E	0.435
F	0.207
G	-1.596

Table 4.5: Parameter Limits in Gas Holdup Correlation (Eqn. 4.12)

Parameter (units)	Range
I	1 or 2
Re	21.63 - 836.49
Ar (x 10^3)	15.6 – 1157.6
U_G/U_L	0 – 9.2
ρ_G/ρ_L (x 10^{-3})	0.147 – 68.9
ρ_P/ρ_L	1.97 – 2.53

Figure 4.15 presents the parity plots between the observed and predicted gas holdups for water at various pressures. The gas holdups at 0.1 MPa are scattered evenly, while at elevated pressures, the gas holdup is consistently overestimated at low holdup conditions, and underestimated at high gas holdup conditions. The correlation produces an overall AARE value of 0.254.

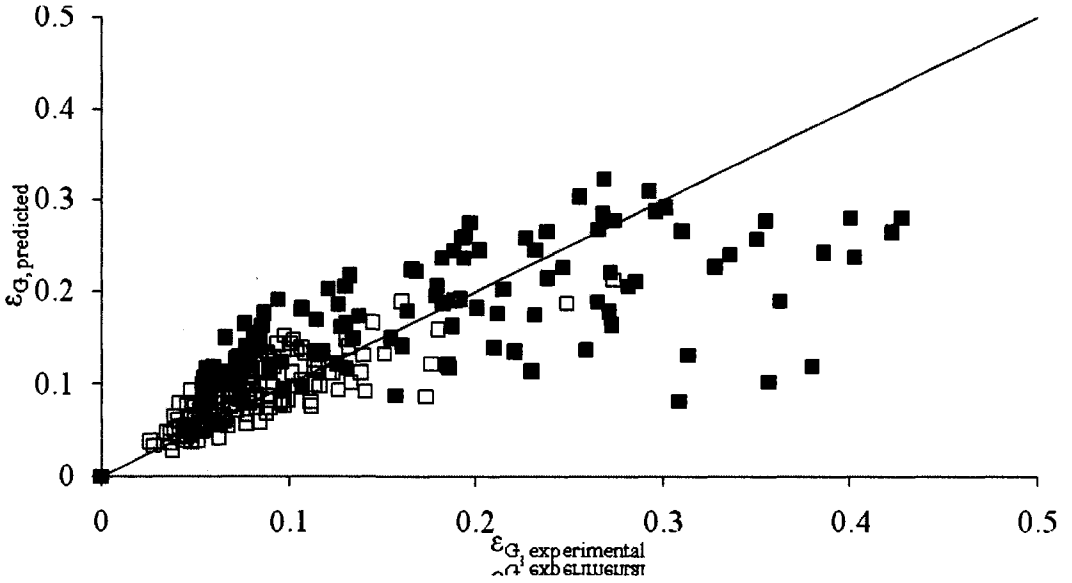

Figure 4.15: Parity Plots Between Observed and Predicted Gas Holdups from Equation (4.12). Open and closed symbols represent atmospheric and elevated pressures, respectively.

4.3.4 Minimum Liquid Fluidization Velocity

Figure 4.16 presents the effect of gas velocity on the minimum liquid fluidization velocity (U_{Lmf}) for water at various pressures. If the fluidization of the particles is dominated by the drag force exerted by the liquid, then the addition of gas will result in

the bed fluidizing at smaller liquid superficial velocities. The effect of the gas velocity on the minimum liquid fluidization eventually wears off at U_G = 0.03 m/s for P = 0.1, at U_G = 0.035 m/s for 1 MPa, and at U_G = 0.047 m/s for P = 4.5 MPa

As seen with all cases of liquid-solid fluidization, pressure has an insignificant effect on the minimum liquid fluidization velocity. As gas is initially introduced, the reduction in U_{Lmf} is not affected by pressure, as an increase in pressure will not significantly reduce the equilibrium bubble size. The effect of pressure on the U_{Lmf} becomes pronounced at higher gas velocities, where at high pressures, the gas bubbles still flow in the dispersed bubbling regime. The solid line is the prediction of the liquid-buoyed/gas-perturbed model from Zhang *et al.* (1995) with constants C_1 and C_2 taken from the work of Grace *et al.* (1982). The model slightly underestimates U_{Lmf} in the liquid-solid systems and overestimates in the three-phase system with an AARE of 0.197. The correlation does not account for a change in gas density with pressure.

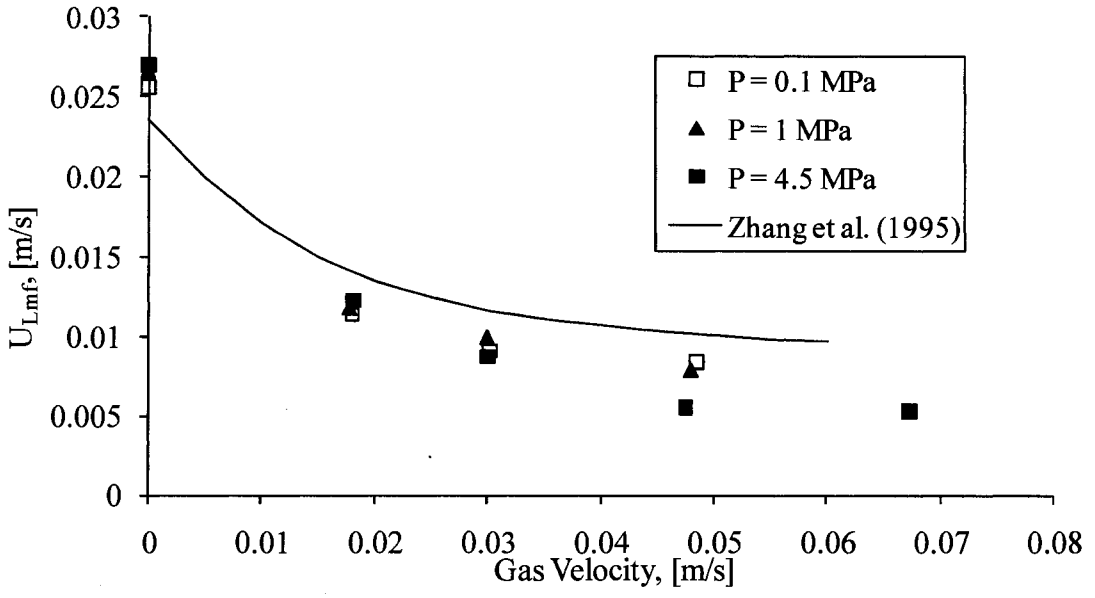

Figure 4.16: Minimum Liquid Fluidization Velocity versus Gas Velocity for Water at Various Pressures

The effect of gas velocity on the minimum liquid fluidization velocity for the 0.5%wt aqueous ethanol solution was not determined. Microbubbles generated by the distributor

create a significant decrease in the U_{Lmf} for the ethanol solution. At a gas velocity of 0.01 m/s, the bed remains fluidized at the lower limit of our liquid velocity measurement of 0.004 m/s. For the liquid-solid system, again there was no effect of pressure on U_{Lmf} and values are similar to those of water as there is not significant effect of surfactant.

Chapter 5 – Conclusions and Recommendations

This work aimed to develop a scaling approach for three-phase fluidized beds operated at elevated pressures, and to evaluate the phase holdups and minimum liquid fluidization velocity for liquid-solid, gas-liquid and gas-liquid-solid fluidized beds at elevated pressures and with a surface-active agent.

It is postulated that the three-phase fluidized bed hydrodynamics can be scaled down based on geometric similarity and dimensional similitude, by matching five dimensionless groups: the liquid Reynolds Number, $Re_L = U_L d_P \rho_L / \mu_L$; the Archimedes Number, $Ar_p = \rho_L g d_P^3 (\rho_L - \rho_G) / \mu_L^2$; a gas-liquid density ratio, ρ_G/ρ_L; a particle-liquid density ratio, ρ_p/ρ_L; and a superficial velocity ratio, U_G/U_L. The main physical properties of the liquid, including the liquid density, viscosity and surface tension, are insufficient to characterize bubble coalescence in multi-component liquids. A bubble coalescence index, I, (1 for mono-component liquids and 2 for multi-component liquids) is an empirical means to account for bubble coalescence inhibition. Experiments were performed with a system composed of 2 mm glass beads, nitrogen gas and a 0.5%wt ethanol aqueous solution, and operated at $0 < U_G < 0.061$ m/s, $0 < U_L < 0.071$ m/s and $0.1 < P < 6$ MPa.

Pressure has no significant effect on the hydrodynamics of liquid-solid fluidized beds. With a mono-component liquid, an increase in pressure results in an increase in the gas holdup in both gas-liquid and gas-liquid-solid fluidized beds. Pressure has a larger effect at lower pressures and eventually an increase in pressure does not significantly increase the gas holdups further. An increase in pressure reduces the equilibrium bubble size. For all conditions, gas holdups in the freeboard region are greater than in the bed.

In a surface-active solution, gas holdups are larger than in the mono-component liquid. In the liquid batch bubble column at pressures larger than 1 MPa, the foam head at the liquid surface became unstable as it continually grew in size. The two-stage gas distribution system affected the initial bubble size in the bed. With a liquid flow, the

shearing effect at the perforated plate created many microbubbles. Due to the numerous small bubbles and the presence of surfactants that inhibited bubble coalescence, there was little effect of pressure over the operating range tested.

Pressure decreases the minimum liquid fluidization velocity for water at large gas velocities, where the flow is still in the dispersed bubbling regime. The effect of pressure is not seen at low gas velocities as bubbles are close to their equilibrium size at all pressures due to the distributor effect. The addition of ethanol resulted in a large decrease in the minimum liquid fluidization velocity. The extent of this effect could not be determined as the bed could not become fixed over the liquid ranged measured by our instrumentation.

Future work should include the continued evaluation of the effects of multi-component liquids on the phase holdups. Experiments operated with particles in the mm-range at elevated pressures should also be evaluated further. The effect of pressure on the holdups of surfactant solutions were masked by the geometry of the gas distribution system. Experiments should be performed with the gas injected independently into the bed above the liquid distributor.

The following is a list of proposed modifications to the high pressure multiphase fluidization unit will help with its operation at elevated pressures:

- The recessed viewing windows are to be made flush with the inner diameter of the column. When operating near the minimum liquid fluidization velocity, particles in the bottom of the window remain unfluidized.
- The column height should be increased to allow for further bed expansions. With the addition of surfactant at elevated pressures, the bed expansion becomes large, and hence the range of gas and liquid flow rates becomes limited.
- The fluid-solid separation (screen) needs to be upgraded. Small particles are capable of being sent out the top of the column. If operating with larger particles, this modification is not necessary.

- The sparger may be placed above the perforated plate to potentially eliminate the strong shearing effect for foaming liquids.
- A liquid cooling system can be added to the system. The liquid pump creates an excess amount of heat and the temperature of the liquid increases significantly, upwards of 7°C per hour.
- The screen in the liquid recycle line should be isolated. The entire line must be removed when the liquid recycle line plugs. By isolating the screen, the removal of particles from the line can be done by a single individual.

Nomenclature

API = American Petroleum Industry gravity = 141/SG(at 60°F) – 131.5, -

Ar_B = bubble Archimedes number = $g\rho_L(\rho_L - \rho_g)d_b^3/\mu_L^2$, -

Ar_P = particle Archimedes number = $g\rho_L(\rho_p - \rho_L)d_p^3/\mu_L^2$, -

Ca_G = Capillary group = $U_G\mu_G/\sigma_L$, -

d_B = diameter of the bubble, m

D_C = column inner diameter, m

d_p = spherical or volume-equivalent particle diameter, m

Eo = bubble Eötvös number = $g(\rho_L - \rho_g)d_b^2/\sigma$, -

Eo* = modified Eötvös number = $g(\rho_L - \rho_g)d_p^2/\sigma$, -

F = wall effect ratio = d_P/D_C, -

Fr_G = gas Froude number = $U_g/\sqrt{gd_p}$, -

g = acceleration due to gravity, m/s^2

H_B = length of bed, m

I = coalescence index, -

M = physical property group (M-group) = $g(\rho_L - \rho_g)\mu_L^4/\rho_L^2\sigma^3$, -

M_A = molecular weight of primary component in Equation (4.7), g/mol

M_B = molecular weight of secondary component in Equation (4.7), g/mol

Mo = Morton number = $g\mu_L^4/\rho_L\sigma_L$, -

M_P = mass of particles in bed, kg

n = Richardson and Zaki exponent in Equation (4.1), -

P = total pressure, MPa

P_S = liquid vapour pressure, MPa

Re_L = liquid Reynolds number = $\rho_L d_p U_L/\mu_L$, -

Re_t = particle terminal velocity Reynolds number = $\rho_L d_p v_t/\mu_L$, -

T = temperature, K

U_G = superficial gas velocity, m/s

U_L = superficial liquid velocity, m/s

U_{Lmf} = minimum liquid superficial velocity, m/s

U_i = intercept liquid velocity from Richardson and Zaki equation at $\varepsilon_L = 1$ from log-log plot, m/s

v_t = particle terminal velocity, m/s

We_M = modified Weber number $= U_L^2 \rho_L D_c / \sigma$, -

X_{GL} = Inertial Lockhart-Martinelli ratio = $\rho_G U_G^2 / \rho_L U_L^2$, -

X_W = weight fraction of the primary liquid in the mixture (w/w), -

Greek Letters

α = parameter in Equation (4.10), -

β = parameter in Equations (4.6) and (4.11), -

Γ = gas distributor parameter used in Equation (1.1), -

δ = parameter in Equation (4.6), -

$-\Delta P$ = dynamic pressure drop = $-\Delta P_T - g\rho_L \Delta z$, Pa

$-\Delta P_T$ = Total pressure drop = $g\Delta z\,(\varepsilon_g \rho_g + \varepsilon_L \rho_L + \varepsilon_s \rho_p)$, Pa

$\Delta\rho$ = density difference between liquid and gas phases, kg/m^3

Δz = vertical distance between taps for differential pressure measurement, m

ε_G = gas holdup, -

ε_L = liquid holdup, -

ε_S = solid holdup, -

μ_L = liquid viscosity, Pa·s

π = dimensionless number, -

ρ_G = gas density, kg/m^3

$\rho_{G,\,STP}$ = gas density at standard temperature and pressure, kg/m^3

ρ_L = liquid density, kg/m^3

ρ_P = particle density, kg/m^3

σ_L = liquid surface tension, mN/m

References

Athabasca Regional Issues Working Group, *Facts Sheet*, Fort McMurray, Alberta (2005).

Athabasca Regional Issues Working Group, *Facts Sheet*, Fort McMurray, Alberta (2001).

Bach, H.F., Pilhofer, T., *Variation of Gas Holdup in Bubble Columns with Physical Properties of Liquids and Operating Parameters of Columns*, German Chemical Engineering, 1, 270-275 (1978).

Behkish, A., Lemoine, R., Oukaci, R., Morsi, B.I., *Novel Correlations for Gas Holdup in Large-Scale Slurry Bubble Column Reactors Operating Under Elevated Pressures and Temperatures*, Chemical Engineering Journal, 115, 157-171 (2006).

Bhatia, V.K., Epstein, N., *Fluidization and Its Applications*, ed. by H. Angelino, J.P. Couderc, H. Gilbert, and C. Laguerie, Cepadues-Editions, Toulouse, 380-392 (1974).

Brue, E., Brown, R.C., *Use of Pressure Fluctuations to Validate Hydrodynamic Similitude in Fluidized Media: Bubbling Beds*, Powder Technology, 119, 117-127 (2001).

Dargar, P., *The Effect of Surfactants on the Hydrodynamics of Bubble Columns and Three-Phase Fluidized Beds*, MASc Dissertation, University of Ottawa, (2005).

Fan, L.S., Yang, W.C., Chapter 27 in *Handbook of Fluidization and Fluid-Particle Systems*, Siemens Westinghouse Power Corporation, Pittsburgh, PA (2003).

Fan, L.S., *Gas-Liquid-Solid Fluidization Engineering*, Butterworth Publishers, Boston, MA (1989).

Gorowara, R.L., Fan, L.S., *Effect of Surfactants on Three-Phase Fluidized Bed Hydrodynamics*, Industrial and Engineering Chemistry Research, 29, 882-891 (1990).

Grace, J.R., *Fluidized-Bed Hydrodynamics*, in Handbook of Multiphase Systems, Ed. Hetsroni, G, Hemisphere, Washington, 8:5-64 (1982).

Han, J.H., Wild, G., S.D. Kim, *Phase Holdup Characteristics in Three-Phase Fluidized Beds*, Chemical Engineering Journal, 43, 67-73 (1990).

He, Y.L., Lim, C.J., Grace, J.R., *Scale-Up Studies of Spouted Beds*, Chemical Engineering Scientific, 52, 329-339 (1997).

Jin, G., *Multi-Scale Modeling of Gas-Liquid-Solid Three-Phase Fluidized Beds Using the EMMS Method*, Chemical Engineering Journal, 117, 1-11 (2006).

Khan, A.R., Richardson, J.F., *Fluid-Particle Interactions and Flow Characteristics of Fluidized Beds and Settling Suspensions of Spherical Particles*, Chemical Engineering Communications, 78, 111-130 (1989).

Kehlenbeck, R., Yates, J., Di Felice, R., Hofbauer, H., Rauch, R., *Novel Scaling Parameter for Circulating Fluidized Beds*, American Institute of Chemical Engineers Journal, 47, 582-589 (2001).

Larachi, F., Belfares, L., Iliuta, I., Grandjean, B.A., *Three-Phase Fluidization Macroscopic Hydrodynamics Revisited*, Industrial and Engineering Chemistry Research, 40, 993-1008 (2001).

Lin, T.J., Tsuchiya, K., L.S. Fan, *Bubble Flow Characteristics in Bubble Columns at Elevated Pressure and Temperature*, American Institute of Chemical Engineers Journal, 44, 545-560 (1998).

Liu M., Li, J., Mwauk, M., *Application of the Energy-Minimization Multi-Scale Method to Gas-Liquid-Solid Fluidized Beds*, Chemical Engineering Science, 56, 6805-6812 (2001).

Luo, X., Lee, D.J., Lau, R., Yang, G., Fan, L.S., *Maximum Stable Bubble Size and Gas Holdup in High-Pressure Slurry Bubble Columns*, American Institute of Chemical Engineers Journal, 45, 665-680 (1999).

Luo, X., Jiang. P.,L.S. Fan, *High-Pressure Three-Phase Fluidization: Hydrodynamics and Heat Transfer*, American Institute of Chemical Engineers Journal, 43, 2432-2445 (1997).

Macchi, A., D*imensionless Hydrodynamic Simulation of High Pressure Multiphase Reactors Subject to Foaming*, PhD Dissertation, University of British Columbia (2002).

McKnight, C.A., Hackman, L.P., Grace, J.R., Macchi, A., Kiel, D., Tyler, J., *Fluid Dynamic Studies in Support of an Industrial Three-Phase Fluidized Bed Hydroprocessor*, The Canadian Journal of Chemical Engineering, 81, 338-350 (2003).

Nacef, S., *Hydrodynamique des Lits Fluidises Gaz-Liquide-Solide: Effets du Distributeur et de la Nature du Liquide*, PhD Dissertation, L'Institut National Polytechnique de Lorraine (1991).

Richardson, J.F., W.N. Zaki, *Sedimentation and Fluidization: Part 1*, Trans. Inst. Chem. Eng., 32, 35-52 (1954).

Ruiz, R.S., Alonso, F., Ancheyta, J., *Effect of High Pressure Operation on Overall Phase Holdups in Ebullated-Bed Reactors*, Catalyst Today, 265-271 (2004).

Safoniuk, M., *Dimensional Similitude and the Hydrodynamics of Three-Phase Fluidized Beds*, PhD Dissertation, University of British Columbia, (1999).

Sinha, T.V., Butensky, M.S., Hyman, D., *Comparison of Cylinders and Spheres in Three-Phase Fluidization*, American Chemical Society, 25, 321-324 (1986).

Song, G.H., Bavarian, F., Fan, L.S., Buttke, R.D., Peck, L.B., *Hydrodynamics of Three-Phase Fluidized Bed Containing Cylindrical Hydrotreating Catalysts,* The Canadian Journal of Chemical Engineering, 67, 265-275 (1989).

Syncrude, *Fact Sheets*, Fort McMurray, Alberta (2005).

Wild, G.,Poncin, S., *Hydrodynamics*, Chapter 1 in *Three-Phase Sparged Reactors*, K.D.P Nigam and A.Shumpe, Eds., Gordon and Breach Publishers, Netherlands, 11-112 (1996).

Wilkinson, P.M., L.L. van Dierendonk, *Pressure and Gas Density Effects on Bubble Break-Up and Gas Hold-Up in Bubble Columns*, Chemical Engineering Science, 45, 2309-2315 (1990).

Zhang J.P., Epstein N., Grace J.R., Zhu J., *Minimum Liquid Fluidization Velocity of Gas-Liquid Fluidized Beds*, Chemical Engineering Research and Design, 73, 347-353 (1995).